

1964

Adaptive sampling in digital control

Kenneth Allen McCollom
Iowa State University

Follow this and additional works at: <https://lib.dr.iastate.edu/rtd>



Part of the [Electrical and Electronics Commons](#)

Recommended Citation

McCollom, Kenneth Allen, "Adaptive sampling in digital control " (1964). *Retrospective Theses and Dissertations*. 3822.
<https://lib.dr.iastate.edu/rtd/3822>

This Dissertation is brought to you for free and open access by the Iowa State University Capstones, Theses and Dissertations at Iowa State University Digital Repository. It has been accepted for inclusion in Retrospective Theses and Dissertations by an authorized administrator of Iowa State University Digital Repository. For more information, please contact digirep@iastate.edu.

This dissertation has been 65-3804
microfilmed exactly as received

McCOLLUM, Kenneth Allen, 1922-
ADAPTIVE SAMPLING IN DIGITAL CONTROL.

Iowa State University of Science and Technology
Ph.D., 1964
Engineering, electrical

University Microfilms, Inc., Ann Arbor, Michigan

ADAPTIVE SAMPLING IN DIGITAL CONTROL

by

Kenneth Allen McCollom

**A Dissertation Submitted to the
Graduate Faculty in Partial Fulfillment of
The Requirements for the Degree of
DOCTOR OF PHILOSOPHY**

Major Subject: Electrical Engineering

Approved:

Signature was redacted for privacy.

In Charge of Major Work

Signature was redacted for privacy.

Head of Major Department

Signature was redacted for privacy.

Dean/of Graduate College

**Iowa State University
Of Science and Technology
Ames, Iowa**

1964

TABLE OF CONTENTS

	Page
I. INTRODUCTION	1
II. REVIEW OF LITERATURE	4
III. METHOD OF INVESTIGATION	10
A. State Variable Technique	11
1. Recursion formula	15
2. Piecewise constant inputs	17
B. Adaptive Sampling Technique	19
1. Prediction equations for unit block	21
2. Design parameters	26
C. Nonlinear, Time-varying Systems	54
IV. EXPERIMENTAL IMPLEMENTATION	57
A. Description of Process System	57
B. Derivation of Mathematical Model	60
1. Dynamics of sample radioactivity	62
2. Dynamics of sample transport	65
3. Dynamics of mass isotope separator	72
4. Combined dynamics at the target	75
C. Solution for System Equations	79
D. System Control	84
1. Multilevel control equations	85
2. Application of adaptive sampling	93
V. CONCLUSIONS AND RECOMMENDATIONS	102
VI. BIBLIOGRAPHY	105
VII. ACKNOWLEDGEMENTS	107

I. INTRODUCTION

Conventional automatic control has made significant accomplishments in industrial and military applications. This type control is the design of control systems to determine the compensation necessary to fulfill a certain set of requirements. The most common requirements are values of gain margin, phase margin, M-peak, rise time, settling time, peak overshoot, integral square error, and mean square error.

Following many years of active development, conventional automatic control system design appears to be approaching a saturation point which, in turn, is encouraging the development of new theories of control. Perhaps the greatest impetus for this change has been the computational aid supplied by modern digital computers. Some of the new mathematical techniques in the developing theories, such as dynamic programming, are impractical without the speed and capacity for calculations now available.

The new techniques in control system design usually use the differential equations that describe the process mathematically as a means for predicting what will happen in the future. Then the predicted values are used to determine present control inputs or sequence of inputs. This mathematical technique is commonly referred to as the "state variable technique" by control engineers. The value of a state is

usually the value of the variable in a first order differential equation describing a portion of the process. If the process is described by an n^{th} order differential equation, then it has n states which are normally determined in the control problem.

The digital computer is not only aiding in the development of such new theories but also is practically and, just as important, economically implementing the theory by acting as an element in the feedback loop of the control systems. The economic advantage has resulted from two sources: first the cost of the computer hardware has declined to reasonable values for use as control elements, and second the hardware and software for computers has developed so that a single computer can be shared by a number of different, otherwise unrelated, experiments.

The purpose of this dissertation is to determine when attention is necessary for the control of an experiment from the computer which is shared with other experiments. To allow investigation of the dynamic behavior of a process a unit block which represents a first order differential equation has been selected. Using deterministic inputs as driving functions the characteristics of the unit block are determined for a variety of inputs. A process system is investigated by building up the complete system from the unit blocks. The state variable technique predicts the output of a unit block

exactly with a piecewise constant input and approximately with a time-varying input.

The error and deviation design curves for a number of different deterministic inputs to the unit block are used in the design of a multivariable control system for a nuclear physics experiment. A sample is irradiated in a nuclear reactor, and the decay characteristics of the radioactive atoms produced are examined. The sample is solid, but through controlled heating its vapor is continuously removed from the reactor and inserted into the ion source of a mass isotope separator. The mass isotope separator separates the radioactive atoms from the parent atoms so that the decay characteristics can be investigated. The control requirement is to supply the same number of atoms in a continuous stream from the reactor as are decaying at the isotope separator target. The system is described by a set of nonlinear differential equations with time-varying coefficients and transport lags. The set of differential equations representing the system can be uncoupled to allow sequential solution of subsets that are linear.

II. REVIEW OF LITERATURE

Prior to 1950, little was published in the area of analysis and design of sampled-data systems. Digital computers were first used in control systems and later used in complex automatic tracking systems for satellites in space. The new emphasis on sampled-data systems has resulted in books devoted solely to the subject (12, 16, 18, 19) instead of chapters in the back of books otherwise devoted to continuous control systems.

The design and synthesis of sampled-data control systems can be divided into several categories. To aid in developing the ideas for this dissertation, the categories here are designated instantaneous feedback control systems and predictive control systems. The instantaneous feedback control system compares the present condition of the output to the desired output and makes a correction to the system. The predictive control system, using the immediate system condition and the expected inputs, predicts what the output will be at some future time and makes a correction as soon as possible following the calculations.

The instantaneous feedback control system was developed first as sampled-data systems came into common use. The most popular technique used to analyze these systems is the Z-transform method (3, p. 272). The use of the Z-transformation

for sampled-data systems is entirely analogous to the application of the Laplace transformation to continuous-data systems. Most of the techniques used for solving linear continuous-data systems, such as the Nyquist criterion, root locus diagram or Bode diagram, can be modified and extended to the studies of linear sampled-data systems (12).

The predictive control systems predict the state of the system at some future time using difference and state variable equations derived from the differential equations describing the physical system. In some sampled-data system design books (16) no distinction is made between the state of a difference equation that is an approximation to the solution of the differential equation and the state variable equation that is an exact solution to the differential equation. A careful documentation of the history of the state variable method as developed by both mathematicians and engineers has been made by Fuller (5).

Kalman and Bertram (10) have presented a general synthesis procedure for using the state variable technique in the design of a control system. However, the final control system uses present values of the states for control of the system. Use of the state variable technique in the design allows the optimum choice of linear combination of all of the states to be fed back to the input. Once these feedback terms are determined the system works as an ordinary multiloop feedback

controller. The authors do suggest that transport lags may be handled in the system using prediction. The digital computer is used for solving the prediction equations after each sample.

Dynamic programming theory applied to the optimum design of digital control systems (1, 2, 19) uses prediction by the state variable method in a multistage decision process to maximize the total return for a system. A systematic solution procedure may be derived by making use of Bellman's (1) Principle of Optimality which states that "an optimal policy has the property that whatever the initial state and the initial decisions are, the remaining decisions must constitute an optimal policy with regard to the state resulting from the first decision." This approach implies that to solve a specific optimization problem the original problem is imbedded within a family of similar problems. The original multistage optimization problem is replaced by a sequence of single-stage decision processes which are easier to handle. The disadvantage is in checking all possible sequences of inputs to obtain the optimum one from each succeeding state. The number of possible paths increases with each succeeding stage. Considerable computer storage is required to check every path and to allow a choice of the one which fits most satisfactorily the particular system.

A predictive control system utilizing dynamic programming has been designed by Chestnut, Sollicito and Troutman (4)

using a two-level "bang-bang" type servo. The number of possible branches of input sequences are reduced considerably when just four inputs are all that are available for choice. The input variable operating the controlled system is actuated by an estimate of the error which will exist at some future time. Repeated estimations of the future error are obtained by predicting ahead, on a fast time base, both the reference and the controlled variable as well as some of their lower order derivatives. The input signal is switched at the time when the predicting computations determine that future synchronization of reference and output would occur if polarity of the input signal were switched at that time.

The state of a linear system can theoretically be changed to any other desired state by putting an impulse into the state. Sufficient energy must be given by the impulse to the system in zero time to change the state. Optimum control is no longer a multistep requirement but can be obtained in a single step at any time. Gupta and Hasdorff (6) have made the technique practical by assuming that the input is a combination of a Gaussian (normal) shaped function and its derivatives. The normal function in the limit as the standard deviation goes to zero is the impulse function. With the normal function the energy does not have to be delivered in zero time. A basic difficulty is generating these normal functions, but it is at least possible. The time required to

change the state is a function of the standard deviation which is made as small as possible.

In many sampled-data control systems signals are sampled periodically, although this type of sampling may not always be possible and in some situations may not be desirable. The introduction of aperiodic sampling may even improve the system stability (12, p. 370). Recently a great increase of interest has occurred in systems in which the sampling operations may not be performed synchronously. Attempts have been made to modify and use some of the methods for handling nonlinear control systems such as describing functions or modifying the Z-transform (9). These methods lead to complex analysis for even simple systems.

Kalman and Bertram (11) have made a major contribution in sampled-data analysis and control by showing how the state variable technique can handle sampling systems of a general type in a clear and uniform way. They claim that the method yields simplifications even in the analysis and synthesis of conventional periodic sampling systems. The method automatically eliminates one of the chief difficulties of the transform method, namely that it is difficult or cumbersome to obtain information about the behavior of the system at any time other than the sampling instants.

In their general theory, Kalman and Bertram give a very broad intuitive definition of the state of a dynamic element

as "a set of numbers (called state variables) which contain as much information regarding the past history of the element as is required for the calculation of the entire future behavior of the element." The evolution of a dynamic system through time may be visualized as a succession of state transitions. Since each transition is independent of everything except the present state and the input during the present transition, then the non-uniform sample period is handled as easily as the uniform sample period. An important characteristic of the state variable technique is that design effort is on the analytical aspects of system problems with the drudgery of numerical computations necessarily left to be performed by a digital computer. The computations performed by the digital computer after a sampling instant are usually quite short compared to the time between two samples. Since this time is usually also short compared to the time constants in the system dynamics, the delay caused by the computations may be disregarded altogether.

For simplicity, Kalman and Bertram use sample and hold elements and assume that the input to the system is piecewise constant. Any input that is varying can be integrated, if known beforehand, through the convolution integral with the transition matrix. The exact value of the input as a function of time in the future must be known for this to be an exact solution.

III. METHOD OF INVESTIGATION

The extent to which system design can proceed in a logical, systematic, and intelligent manner is to a degree measured by the knowledge of the process dynamics. Thus, the first goal in control system design must be the determination of the dynamic characteristics of the process to be controlled. The dynamic characterization of a process is commonly described by a set of first order differential equations which are functions explicitly of time and functions of the plant states, $x(t)$; driving control functions, $u(t)$; and disturbance functions, $n(t)$.

In vector form,

$$\dot{\bar{x}}(t) = \bar{f}[\bar{x}(t), \bar{u}(t), \bar{n}(t), t] \quad (1)$$

In addition to this general equation the process usually has limits on the permissible driving functions because of practical considerations such as saturation or power limitation.

The mathematical model of a system may be made up of differential equations with order greater than one. Fortunately, equations of higher order can always be treated numerically by reducing them to a larger system of first order equations of the form of Equation 1. Henrici (7) has shown that such reduction does not increase discretization error in digital solutions. Since the state variable method requires

system equations to be first order, the model must first be reduced to a first order set of differential equations.

A. State Variable Technique

The class of control systems which have received considerable attention in the literature are those described by the following vector form of the differential equations.

$$\dot{\bar{x}}(t) = A(t)\bar{x}(t) + \bar{u}(t) + \bar{n}(t) \quad (2)$$

where $A(t)$ is referred to as the coefficient matrix of the process. This process is said to be linear and non-stationary. However, the process is linear and stationary if $A(t)$ is not a function of time. For the latter case, consider the solution to the homogeneous vector equation where there are no driving functions or disturbances to the system. Thus

$$\dot{\bar{x}}(t) = A \bar{x}(t) \quad (3)$$

The plant starts to move at time, t_0 , from an initial state, \bar{x}_0 . The solution of this homogeneous vector differential equation is similar to the solution of a single first order differential equation

$$\dot{x}(t) = m x(t) \quad (4)$$

Equation 4 has the solution

$$x(t) = e^{m(t-t_0)} x_0 \quad (5)$$

where m is a constant. In the vector differential Equation 3 the term, A , is a matrix. Before a solution of the vector differential equation can be obtained by analogy to the first order differential equation a definition of exponentiation of a matrix must be made. Since

$$e^{mt} = \sum_{k=0}^{\infty} \frac{m^k t^k}{k!} \quad (6)$$

then let

$$e^{At} = \sum_{k=0}^{\infty} \frac{A^k t^k}{k!} \quad (7)$$

for which there are defined matrix operations. This suggests that the solution for the vector differential equation is

$$\bar{x}(t) = e^{A(t-t_0)} \bar{x}_0 \quad (8)$$

The equation

$$\Phi(t - t_0) = e^{A(t-t_0)} \quad (9)$$

is commonly defined as the transition matrix of the system since

$$\bar{x}(t) = \Phi(t - t_0) \bar{x}_0 \quad (10)$$

shows that if \bar{x}_0 are the states at some initial time, t_0 , the movement or transition of the states to new positions at t is only a function of the initial state and the transition matrix.

The solution of the general differential equation with driving forces and disturbances can be shown to be of the form

$$\bar{x}(t) = \Phi(t - t_0)\bar{c}_1(t) \quad (11)$$

Differentiating with respect to t gives

$$\dot{\bar{x}}(t) = A \bar{x}(t) + \Phi(t - t_0)\dot{\bar{c}}_1(t) \quad (12)$$

Setting this equal to the general form of the differential equation in Equation 2 with A not being a function of time makes the following equality necessary for Equation 11 to be a solution.

$$A \bar{x}(t) + \bar{u}(t) + \bar{n}(t) = A \bar{x}(t) + \Phi(t - t_0)\dot{\bar{c}}_1(t) \quad (13)$$

Cancelling terms and solving for $\dot{\bar{c}}_1(t)$ gives

$$\dot{\bar{c}}_1(t) = \int_{t_0}^t \Phi^{-1}(\tau - t_0) [\bar{u}(\tau) + \bar{n}(\tau)] d\tau + \bar{c}_2 \quad (14)$$

Substituting this into Equation 11 gives the solution as

$$\bar{x}(t) = \Phi(t-t_0)\bar{c}_2 + \Phi(t-t_0) \int_{t_0}^t \Phi^{-1}(\tau - t_0) [\bar{u}(\tau) + \bar{n}(\tau)] d\tau \quad (15)$$

The transition matrix before the integral can be taken inside

the integral sign since it is not a function of the integrating variable. The definition of the transition matrix as an exponential function allows consolidation of the two transition matrices now under the integral sign. In addition, at $t = t_0$ the transition matrix, $\Phi(t - t_0)$, becomes the identity matrix. Therefore the constant C_2 is just the value of $\bar{x}(t_0)$. The final result is

$$\bar{x}(t) = \Phi(t - t_0)\bar{x}(t_0) + \int_{t_0}^t \Phi(t - \tau) [\bar{u}(\tau) + \bar{n}(\tau)] d\tau \quad (16)$$

where

$$\Phi(t - t_0) = e^{A(t - t_0)} \quad (17)$$

and the vector form of the equation for which this is the solution is

$$\dot{\bar{x}}(t) = A \bar{x}(t) + \bar{u}(t) + \bar{n}(t) \quad (18)$$

the linear, time-stationary form of Equation 2. This powerful equation expresses the instantaneous motion of the process in terms of the driving control signals, any disturbances and the initial states. These equations describe the exact motion of the process if the original equations are an exact mathematical model of the process and if the control signal, the other driving functions and the disturbances are exactly known. These latter qualifications place rather stringent conditions

on the results. The exactness of this solution is emphasized since the approximate numerical solution of a differential equation is often obtained by solving a related difference equation which results in a state-transition equation similar to Equation 16.

1. Recursion formula

The state variable solution developed in the last section and shown in Equation 16 is more useful for handling in the computer if the equation is placed in a recursive form. This can be accomplished if the prediction period is constant. Disturbances also are assumed to be zero and all inputs are assumed to be deterministic in nature.

Letting the present time be t_k and eliminating the disturbance term as an input to the system, Equation 16 becomes

$$\bar{x}(t) = \Phi(t - t_k)\bar{x}(t_k) + \int_{t_k}^t \Phi(t - \tau)\bar{u}(\tau)d\tau \quad (19)$$

This general form, valid for $t > t_k$, is useful for calculating exact output states where more than one stage is in sequence. However, the recursion equation is obtained by always predicting a fixed period, T , ahead of the present time. Thus, if t is replaced by t_{k+1} then the recursion equation becomes

$$\bar{x}(t_{k+1}) = \Phi(T)\bar{x}(t_k) + \int_{t_k}^{t_{k+1}} \Phi(t_{k+1} - \tau)\bar{u}(\tau)d\tau \quad (20)$$

The following substitution will be useful throughout:

$$T = t_{k+1} - t_k \quad (21)$$

Equation 20 is the equation with which the majority of the future development is involved.

The recursion formula can be used for two different situations that appear in control systems. When the differential equations describing the dynamics of the system are reduced to a set of first order differential equations and states assigned, all of the states will probably not be measurable. If the state cannot be measured, the value of the state at the present is known only through having calculated it in the prediction Equation 20, starting from a known initial condition of the state. Thus, any error in predicting the state T seconds later tends to accumulate as any transient condition persists. A state that cannot be measured is referred to as an inaccessible state, and the state that is measurable is an accessible state. Usually, through careful choice of states, most of the state variables in a system can be measured. Accessibility and inaccessibility are fundamental to the application of the state variable method, since the method requires that the present state be known. Any error in calculating the inaccessible state tends to accumulate during

a transient input condition and disappear during a stable input condition to the state.

Referring again to the recursion Equation 20, the difference in using this equation for calculation of the accessible and the inaccessible states is the value used for $\bar{x}(t_k)$. If the state is accessible, the value of the measurement at t_k for the state variable is used. If the state is inaccessible the previously predicted value for the state is used. The predicted values for the states $\bar{x}(t_{k+1})$ just T seconds later are exact values only if both the present states $\bar{x}(t_k)$ are known and the driving functions $\bar{u}(t)$ are known for the period.

2. Piecewise constant inputs

The state variable technique offers the control engineer a set of tools which allows him to predict the complete state of his process at any future time. The prediction is exact only if he knows the input driving functions to the process from the present to the time of the prediction. If the driving function is under his control, he has no problem. However, there are driving functions that are not under his control and can change at any time. To allow prediction to still be accomplished some type of approximation for the input over the sample period must be made.

The simplest procedure is to assume that the input

driving function remains constant during T in Equation 20. A more sophisticated procedure is to linearly extrapolate the driving function from its value at the preceding time through the value at the initial time and on to a value at the prediction time. An even more intricate procedure is to curve fit the last three input function values and represent the driving function as a polynomial. The last two procedures require considerable computer processing which for a real-time, shared computer could be impractical.

The mathematical form is most simple when the driving functions for a given differential equation in the matrix are measured and are assumed to remain constant at that value over the period of prediction. The amount of error is dependent on how far the driving function changes during the period. By investigating the system it is usually possible to determine how rapidly a driving function can change. For example, if the input to a given differential equation is the output from another state of the system, the time constant for that state, together with its permissible input, will limit the rate of magnitude change possible. Chemical reactions can only progress at certain rates which can be measured and defined. In the system to be considered later, the neutron flux in the reactor will normally change no faster than a certain prescribed rate.

The error involved by assuming that a driving function

remains constant can be investigated. The results can determine the time available for prediction and error correction without exceeding the control specifications of the system.

One fortunate condition exists for the general prediction equation. If the driving function remains constant for several periods, any past errors gradually are reduced to zero. This condition fits nicely the intuitive idea that the most recent measurements should be the ones that more readily indicate the value of the present state and that the measurement made in the more distant past have less and less weight on the value of the present state. Then, if there are no calculation errors for a period of time, the total error diminishes. Choosing the simple approximation of a piecewise constant driving function to all differential equations in the system simplifies the control computations required from the digital computer to a minimum number of simple manipulations.

B. Adaptive Sampling Technique

An adaptive sampling technique is here defined to be that choice of constant prediction period that will satisfy system control specifications over a specified range of system conditions. The complete range of system operation is divided into a number of classes for which criteria can be devised for determining when the system is in each class. In each class

the prediction period is to be no smaller than that required over the range of the operation of the class. The objective for the adaptive sampling is to use the digital computer for control as little as possible yet maintain the system control specifications.

A method is developed here that is general enough to allow use by a control engineer who has, or can develop, an adequate mathematical model for the process. The model is reduced to a set of first order differential equations and then converted to Laplace Transform block diagrams. The knowledge of the behavior of a single first order differential equation, or similarly a single first order Laplace Transform block, for a reasonable number of deterministic inputs allows the control engineer to analyze the control behavior of his complete block diagram one block at a time.

The first order differential equation to be used as the basic building block is given by

$$\dot{x}_1(t) + \frac{1}{\tau_1} x_1(t) = \frac{1}{\tau_1} u_1(t) \quad (22)$$

and the corresponding Laplace Transform unit block is shown in Figure 1. A set of deterministic inputs are also shown in Figure 1. The equations representing these inputs are

$$\text{Ramp:} \quad u_1(t) = t, \quad u_1(t_0^-) = 0 \quad (23)$$

$$\text{Unit step:} \quad u_1(t) = u(t-nT), \quad u_1(t_0^-) = 0, \quad 0 < n < 1 \quad (24)$$

Positive exponential: $u_1(t) = e^{t/\tau_p}, u_1(t_0^-) = 1$ (25)

Unit step with
negative exponential: $u_1(t) = e^{-t/\tau_p}, u_1(t_0^-) = 0$ (26)

Since the differential equation is a linear equation, the principle of superposition applies. The total response of the output for the sum of several inputs at the same time is found by considering each input separately and summing their individual outputs. This allows even more variety in simulating different inputs.

1. Prediction equations for unit block

Two sets of prediction equations are required to allow development of design parameters for decisions for the adaptive sampling. One of the sets of equations is an exact solution for the output of the unit block for a given input. The other set of equations is that which uses piecewise constant approximations for the input and thus obtains an approximate solution for the output of the unit block. This set of equations will later be used as the control equations in the real time digital control. In this section, the approximate solutions are compared to the exact solutions for a given input to generate design parameter curves.

The recursion equation developed earlier and given in vector form in Equation 20 is the equation from which both the exact and the approximate solutions for the output of the unit

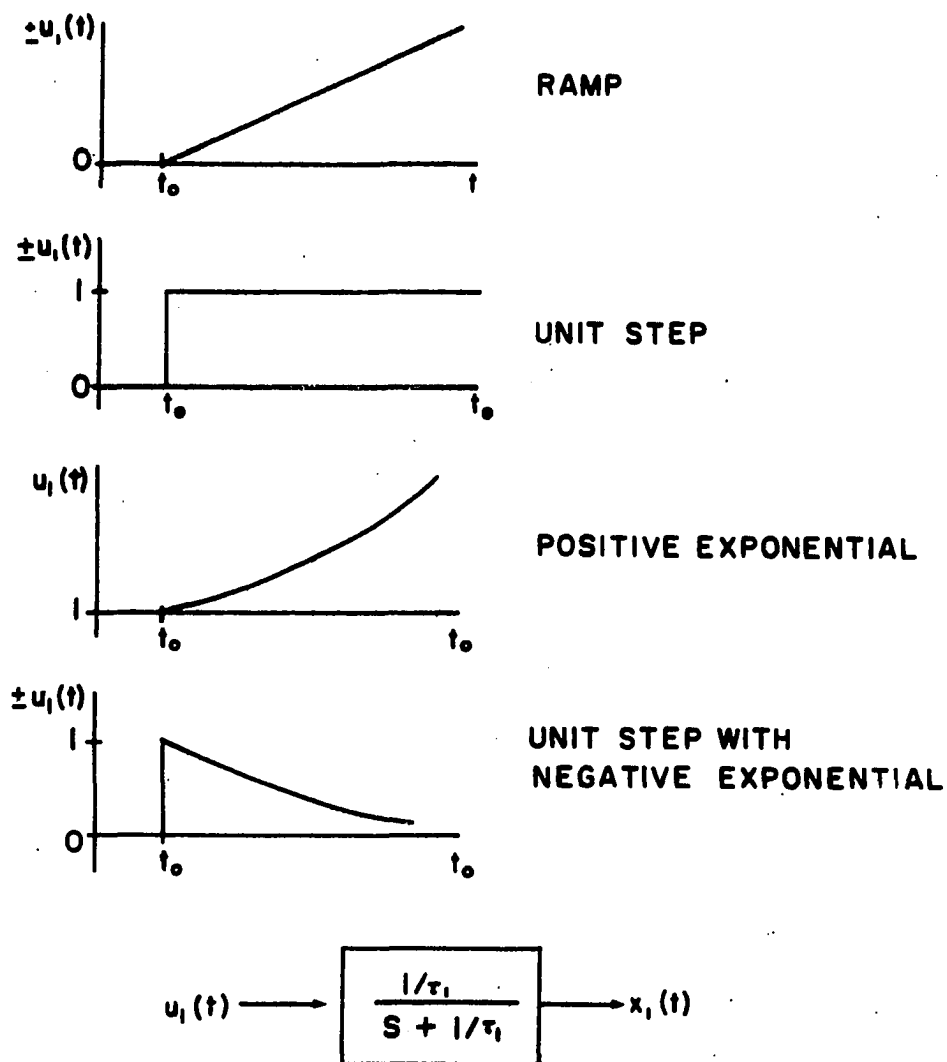


Figure 1. The first order unit block and the input waveforms investigated

block are obtained. For the first order differential equation given in Equation 22, the transition matrix is readily determined from the homogeneous solution to be

$$\Phi(t) = e^{-t/\tau_1} \quad (27)$$

Substituting this into the recursion equation gives

$$x_1(t_{k+1}) = e^{-T/\tau_1} x_1(t_k) + \frac{1}{\tau_1} \int_{t_k}^{t_{k+1}} e^{-(t_{k+1}-\tau)/\tau_1} u_1(\tau) d\tau \quad (28)$$

This equation generates both the exact and the approximate solution for the output when $u_1(t)$ and $u_1(t_k)$, respectively, are used for $u_1(\tau)$ under the integral sign. In the approximate case, $u_1(t_k)$ is no longer a function of the integrating variable, so it can be brought out in front of the integral sign. In the exact case u_1 is a function of the integrating variable so cannot be brought outside of the integral.

The simulation of the unit block is made with K and all inputs set to unity. This allows universal curves to be generated with gain factors inserted by the design engineer for each system investigated. The percent error used for the exponential curves is defined by

$$\text{Percent Error} = \frac{x_1(t_{k+1})_{\text{exact}} - x_1(t_{k+1})_{\text{approx.}}}{x_1(t_{k+1})_{\text{exact}}} \quad (29)$$

The error is evaluated at each step. This definition of error

automatically normalizes the result since all gain factors cancel. The inputs other than the exponential ones use the deviation between the exact and the approximate outputs to allow the generation of useful design curves.

Initiating each of the inputs at the instant of a sample tends to maximize the error presented in the resulting curves. Anytime there has been a choice of doing part of the measurement or calculation two ways, the one causing the most error has been chosen. The resulting curves tend to be pessimistic in their estimate of the error. In the case of the unit step, there is only error in predicting the output between the time the step occurs and the next sample instant, since after that the input is constant. A constant input makes the output prediction for both the approximate and the exact solutions identical.

The prediction equations are obtained by substituting $u_1(t)$ and $u_1(t_k)$, respectively, for each input investigated. Integrating over the recursive limits gives the following set of recursive prediction equations for the unit block transfer function shown in Figure 1:

Case a: $u_1(t) = t$, $u_1(t_0) = 0$, $x_1(t_0) = 0$

Exact solution

$$x_1(t_{k+1}) = e^{-T/\tau_1} x_1(t_k) + (kT - \tau_1)(1 - e^{-T/\tau_1}) + T \quad (30)$$

Approximate solution

$$x_1(t_{k+1}) = e^{-T/\tau_1} x_1(t_k) + kT(1 - e^{-T/\tau_1}) \quad (31)$$

Case b: $u_1(t) = u(t - nT)$, $u_1(t_0^-) = 0$, $x_1(t_0) = 0$

Exact solution,

$$x_1(t_1) = 1 - e^{-(1-n)T/\tau_1} \quad (32)$$

Case c: $u_1(t) = e^{t/\tau_p}$, $u_1(t_0) = 1$, $x_1(t_0) = 1$

Exact solution,

$$x_1(t_{k+1}) = e^{-T/\tau_1} x(t_k) + \frac{\frac{T}{\tau_1}}{\frac{T}{\tau_1} + \frac{T}{\tau_p}} e^{kT/\tau_p} (e^{T/\tau_p} - e^{-T/\tau_1}) \quad (33)$$

Approximate solution,

$$x_1(t_{k+1}) = e^{-T/\tau_1} x_1(t_k) + e^{kT/\tau_p} (1 - e^{-T/\tau_1}) \quad (34)$$

Case d: $u_1(t) = e^{-t/\tau_p}$, $u_1(t_0^-) = 0$, $u_1(t_0^+) = 1$, $x_1(t_0) = 0$

Exact solution,

$$x_1(t_{k+1}) = e^{-T/\tau_1} x_1(t_k) + \frac{\frac{T}{\tau_1}}{\frac{T}{\tau_1} - \frac{T}{\tau_p}} e^{-kT/\tau_p} (e^{-T/\tau_p} - e^{-T/\tau_1}) \quad (35)$$

Approximate solution,

$$x_1(t_{k+1}) = e^{-T/\tau_1} x_1(t_k) + e^{-kT/\tau_p} (1 - e^{-T/\tau_1}) \quad (36)$$

2. Design parameters

The recursion equations describing the exact solution and the approximate solution of the output state for the four input cases are placed in forms that minimize the number of variables. Wherever possible, the sample period and the time constants, τ , were put in ratio form, T/τ . This is a non-dimensional ratio which is easy to use in the general application of these curves. The abscissa of each of the curves generated has been made the ratio of the sample period to the time constant of the unit block, T/τ_1 . The ordinate is either some form of the percent error or the deviation of the approximate value from the exact value of the output state. Finally, the family of curves are generated by the remaining variables in each of the cases. For instance, in all of the exponential inputs, the families of curves are for different values of the ratio of the unit block time constant to the exponential time constant, τ_1/τ_p .

The approximate solution may have either an accessible or an inaccessible output. If the output is accessible, then the present state, $x_1(t_k)$, of the system is obtained from the exact solution when prediction was made from the previous state. The exact solution gives the same result as a measurement does for the present state. If the output is inaccessible, then the present state, $x_1(t_k)$, is obtained from having predicted $x_1(t_{k+1})$ approximately from the previous state.

a. $u_1(t) = t$ The ramp input to the unit block eventually results in a fixed amplitude deviation between the approximate output and the exact output for a given sample period. The time in which the deviation ceases to increase is dependent upon the time constant of the unit block, τ_1 . Since the abscissa of the curves is T/τ_1 a family of curves show the gradual increase in amplitude at each t_k following the initiation of the ramp. Figures 2 and 3 show two different scales for the abscissa and display the deviation of the approximate output from the exact output. The curves designated as t_k show the deviation at the end of the k^{th} period just kT seconds after initiation of the ramp. For the accessible case, the deviation is reduced to zero again at the end of each period by a measurement. The result is that the deviation at the next sample is again the same value as shown at t_1 for a given value of T/τ_1 . Thus, only one curve, that designated t_1 is used for the accessible output state, while all of the curves are used for the inaccessible output state, and the deviation at kT seconds is indicated by the curve designated as t_k . A dashed line in both of the figures indicates the asymptotic value of the deviation at t_{∞} . Since the simulation in the digital computer was carried only to $k = 20$, further specific curves are not included.

b. $u_1(t) = u(t - nT)$ The unit step input to the unit block results in a deviation of the output state at the next sample instant. The deviation is dependent on the time

Figure 2. Amplitude deviation of the approximated output from the actual output state of a unit block at sample instants, t_k , following the initiation of a ramp input. Range 1

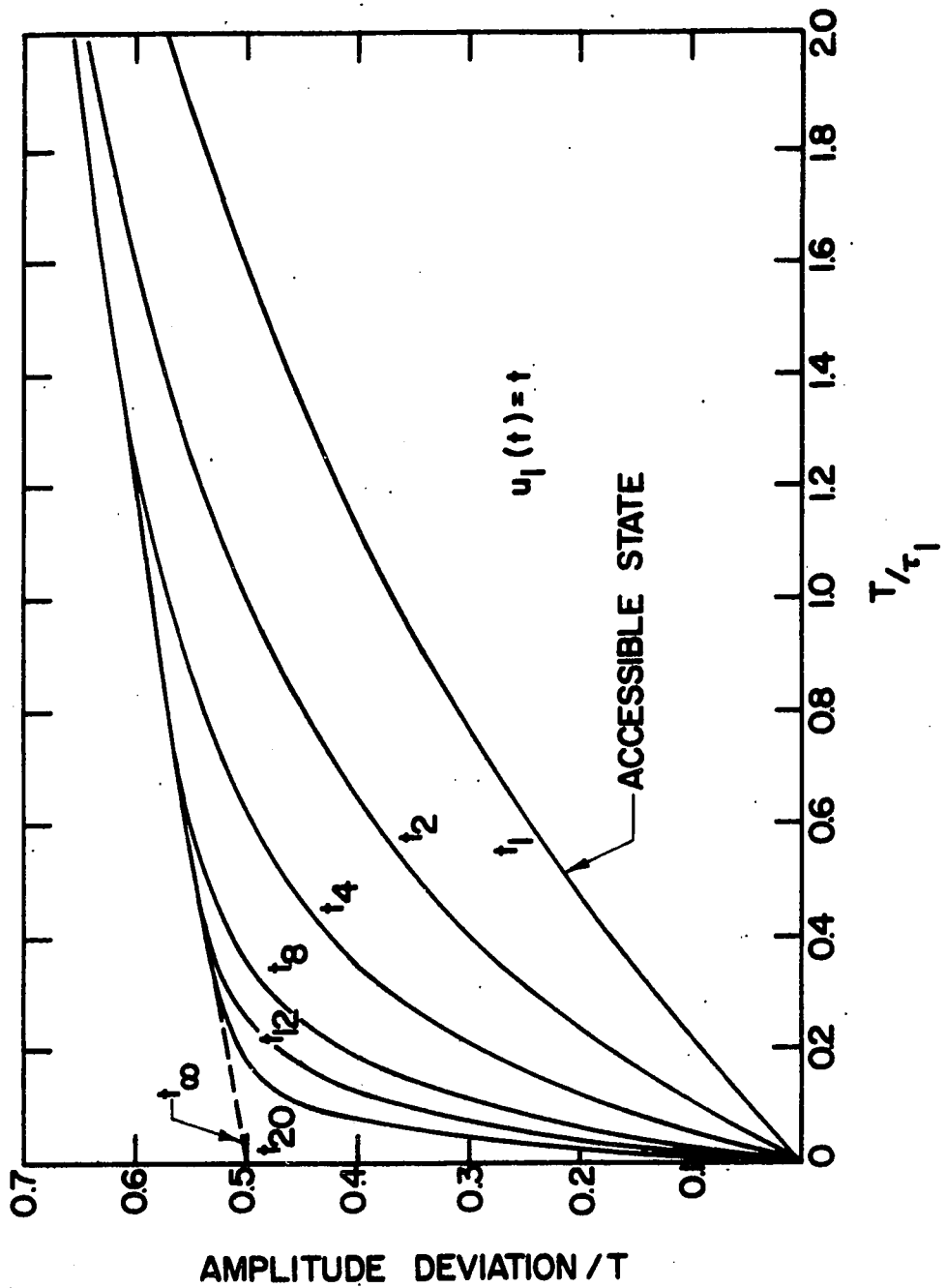


Figure 3. Amplitude deviation of the approximated output from the actual output state of a unit block at sample instants, t_k , following the initiation of a ramp input. Range 2

constant of the unit block. As the sample period is made longer, the output has time to grow larger. The deviation, as a function of T/τ_1 and the time after a sample that the step starts, is shown for two ranges of T/τ_1 in Figures 4 and 5. The parameter, n , varies between 0 and 1 where the step occurs at t_0^+ for $n = 0$ and at t_1^- for $n = 1$. As previously indicated, there is no further deviation between the approximate solution and exact solution for the output after the first sample following the unit step.

c. $u_1(t) = e^{t/\tau_p}$ The positive exponential input to the unit block eventually results in a constant error between the approximate output and the exact output for given T/τ_1 and τ_1/τ_p . The exponential input reaches this asymptotic error in a time dependent on the time constant of the unit block.

Since the abscissa is in terms of T/τ_1 , the small values of the abscissa take more sample periods to reach the asymptotic error. For T/τ_1 greater than 0.5 the asymptotic error is reached in three or four sample periods. The comparisons for the asymptotic errors, resulting for the inaccessible and accessible output states, are shown for two ranges of T/τ_1 in Figures 6 and 7. These two figures are included for comparative purposes only. The inaccessible state for two ranges of T/τ_1 and a more complete selection of ratios, τ_1/τ_p , are given in Figures 8 and 9. Similarly, the accessible output state is covered in Figures 10 and 11. It was not easy to display in a

Figure 4. Amplitude deviation of the output state of a unit block at the next sample instant following the input of a unit step nT seconds after the last sample. Range 1

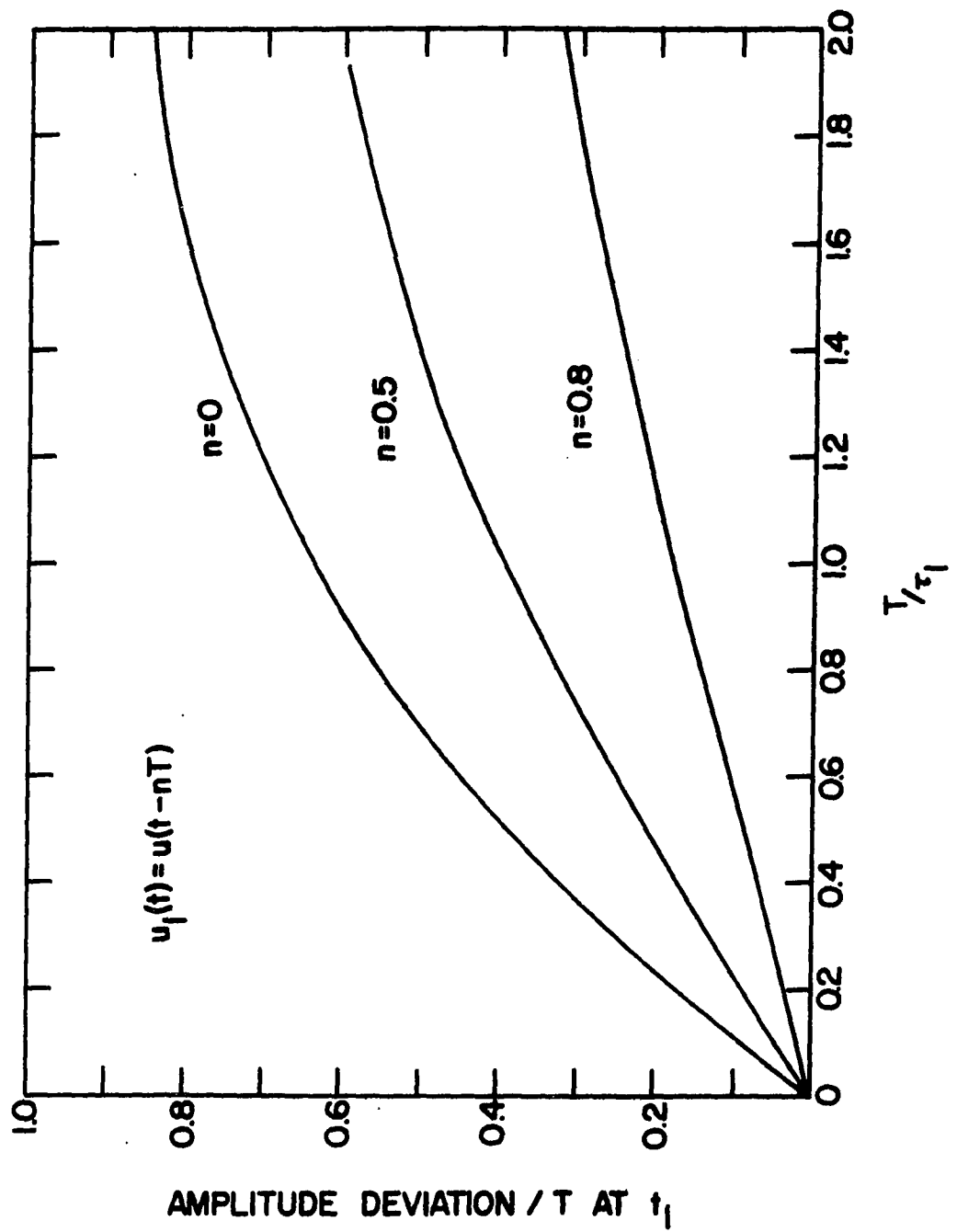


Figure 5. Amplitude deviation of the output state of a unit block at the next sample instant following the input of a unit step nT seconds after the last sample. Range 2

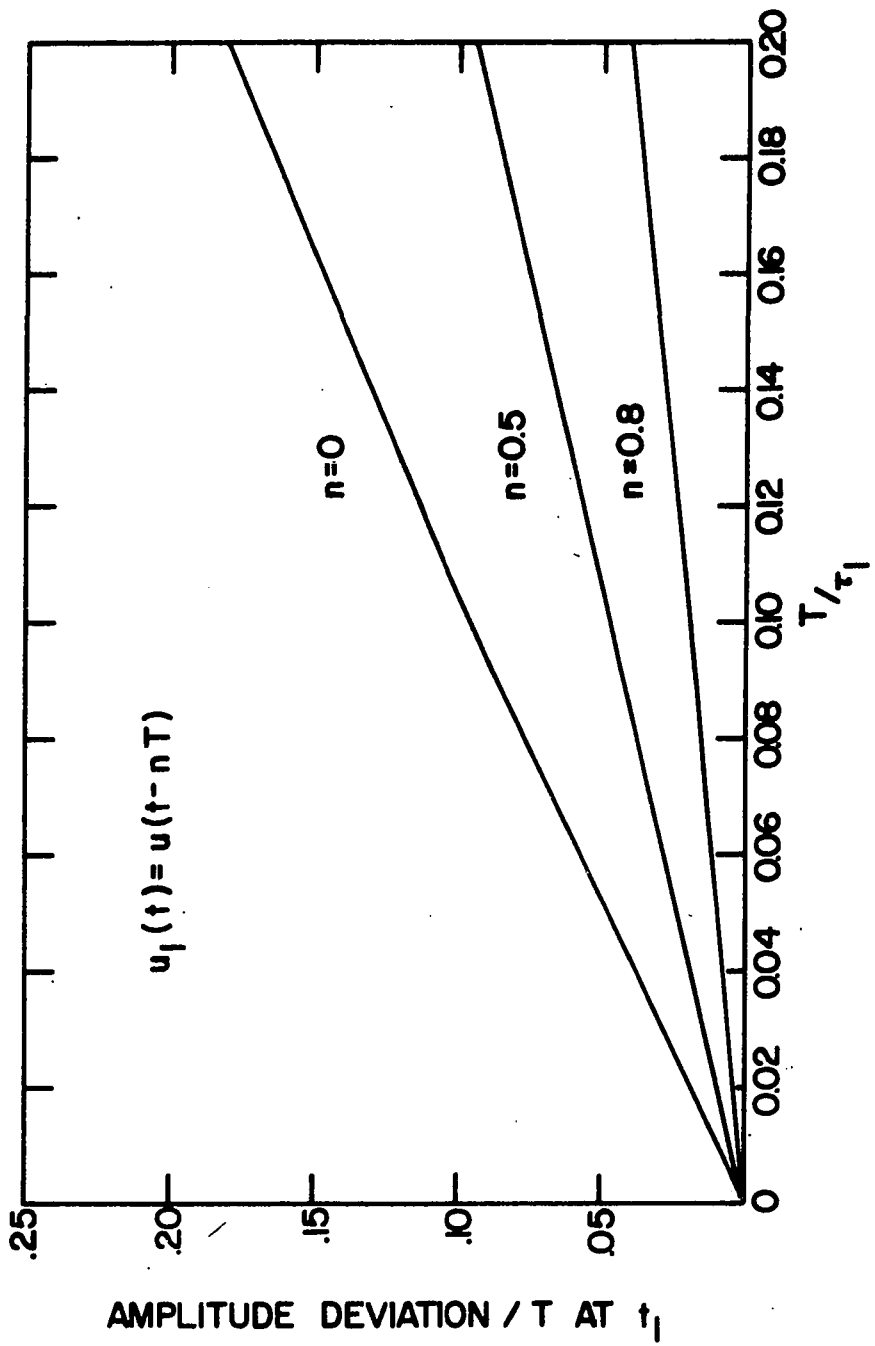


Figure 6. Comparison of approximation errors for the accessible and inaccessible output states of a unit block with a positive exponential input. Range 1

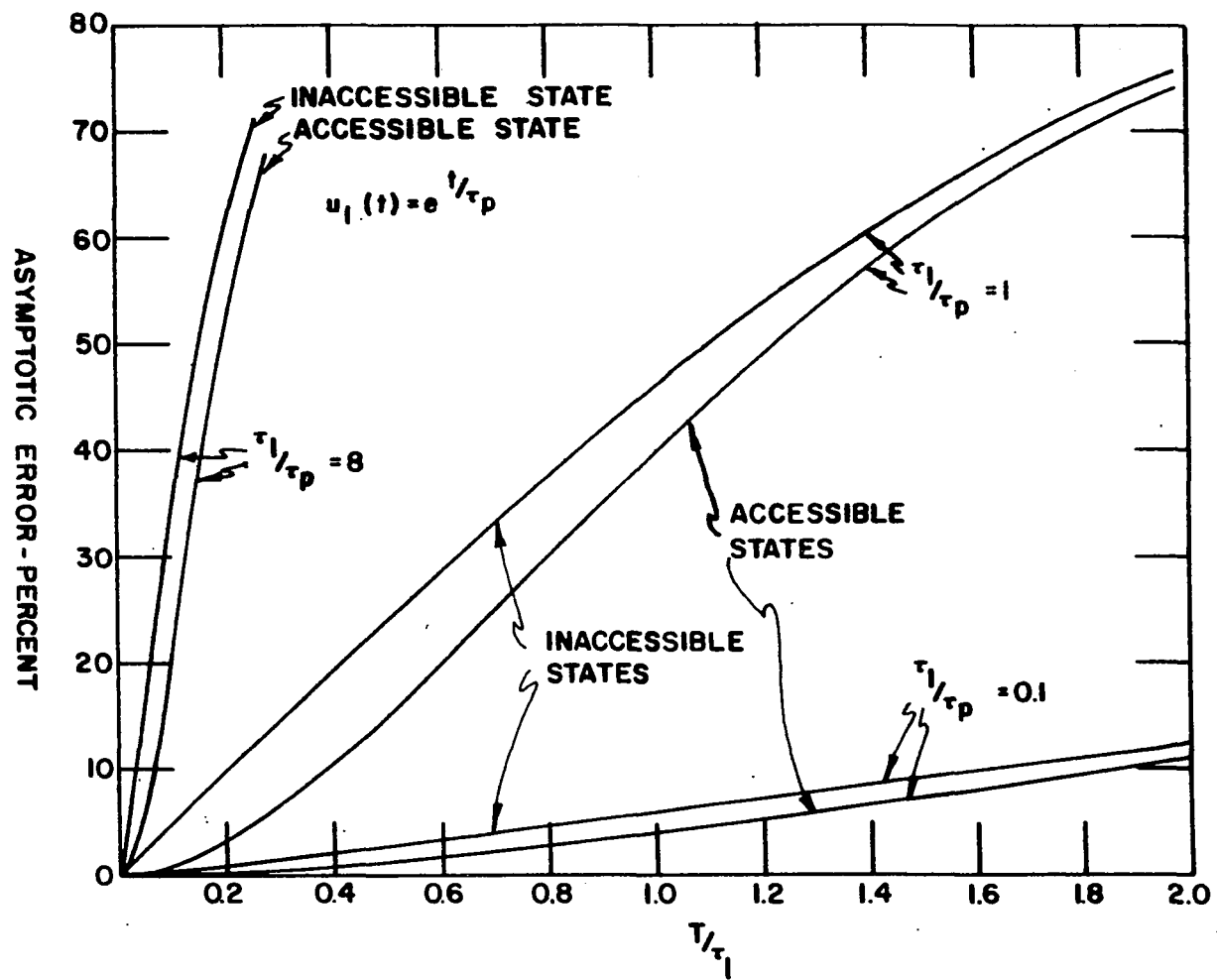


Figure 7. Comparison of approximation errors for accessible and inaccessible output states of a unit block with a positive exponential input.
Range 2

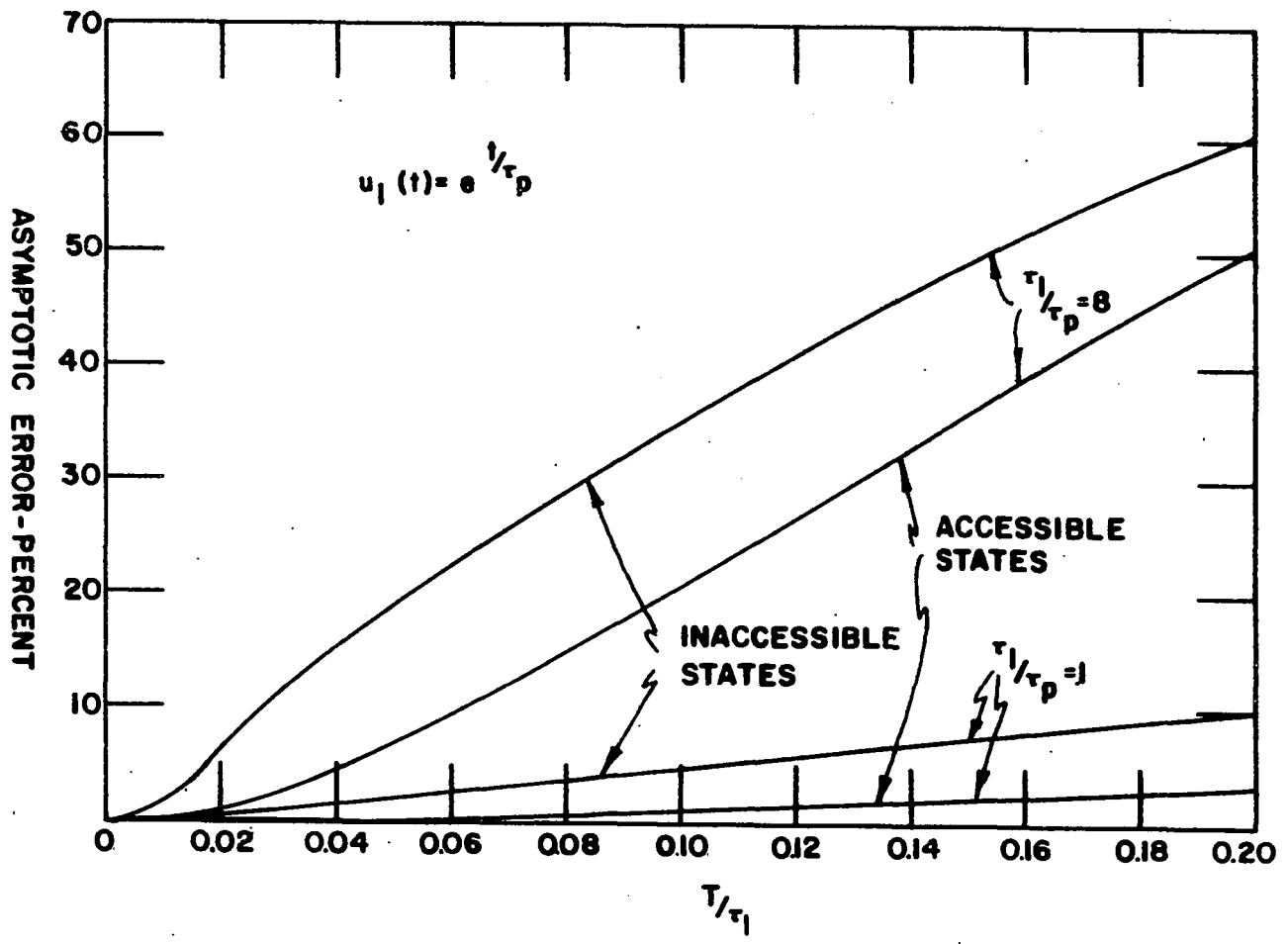


Figure 8. Approximation errors for an inaccessible output state of a unit block with a positive exponential input. Range 1

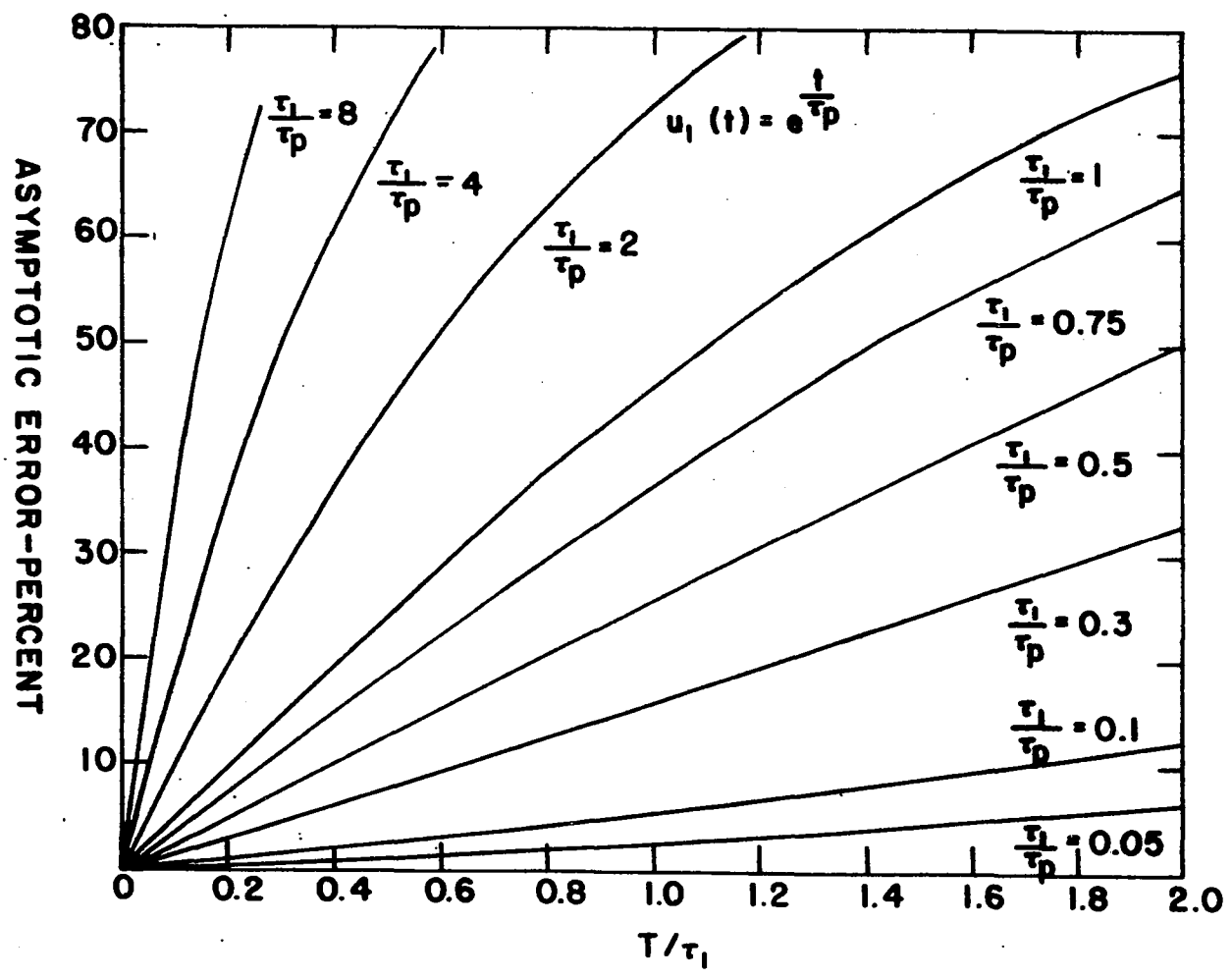


Figure 9. Approximation errors for an inaccessible output state of a unit block with a positive exponential input. Range 2

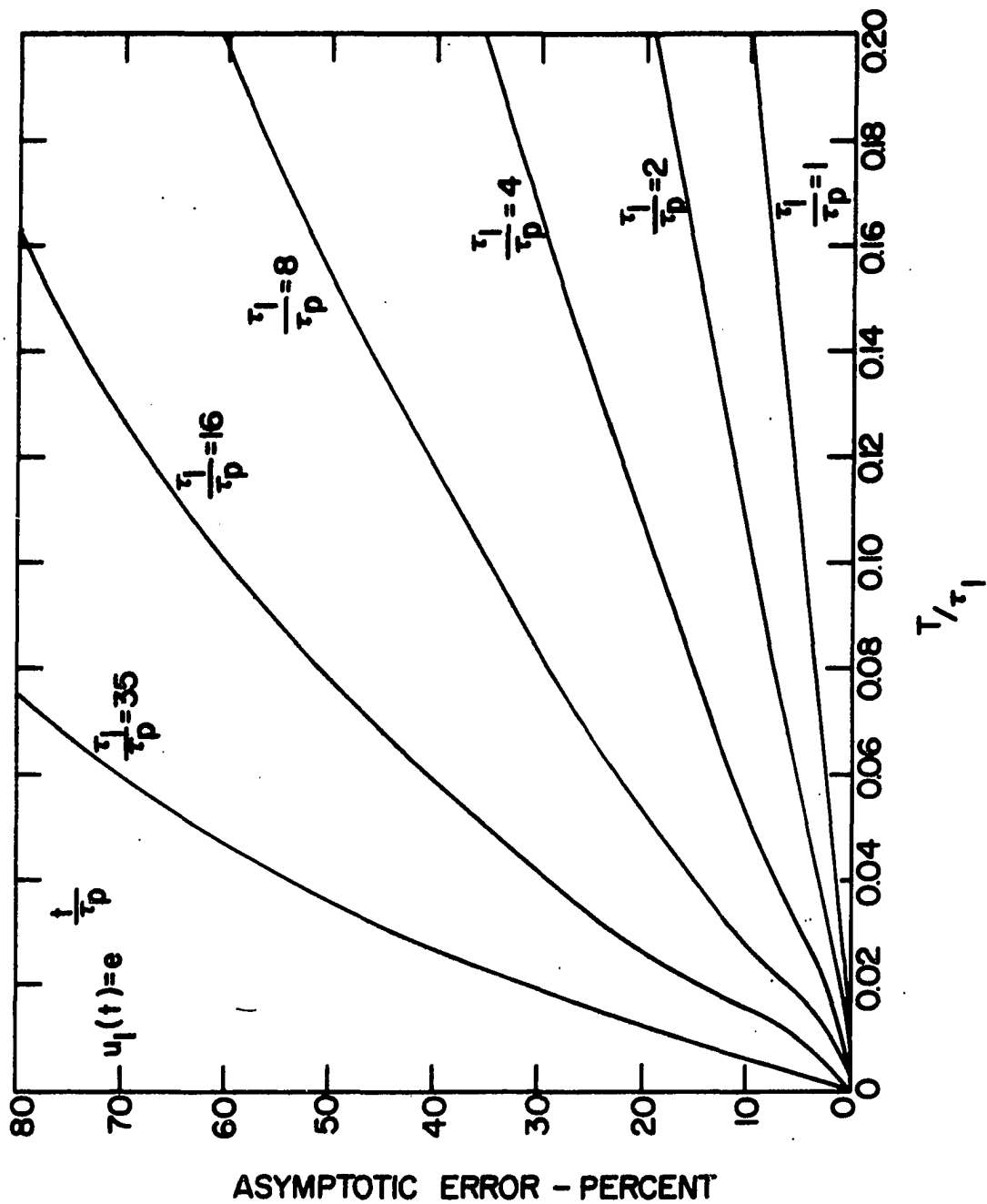


Figure 10. Approximation errors for an accessible output state of a unit block with a positive exponential input. Range 1

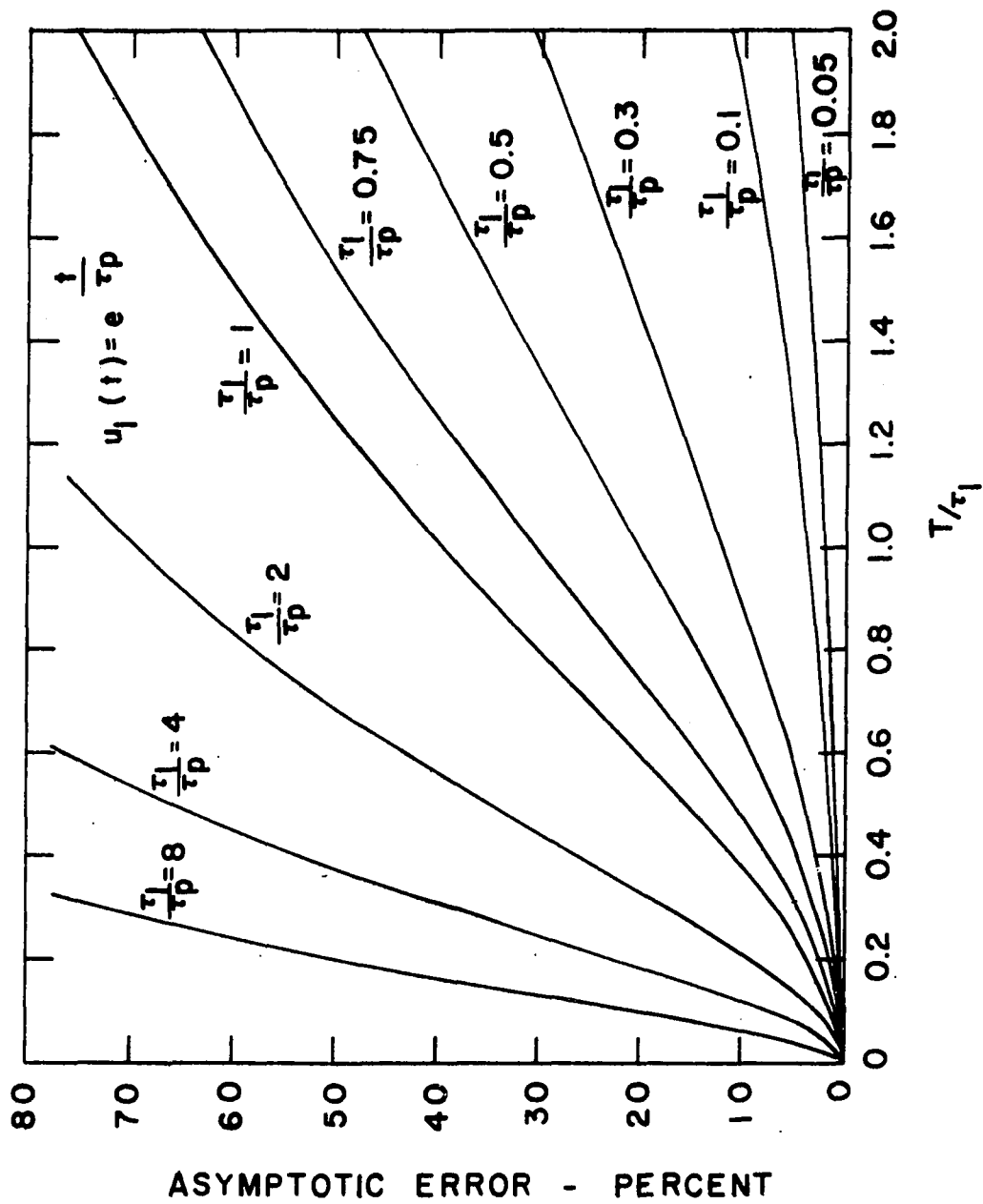
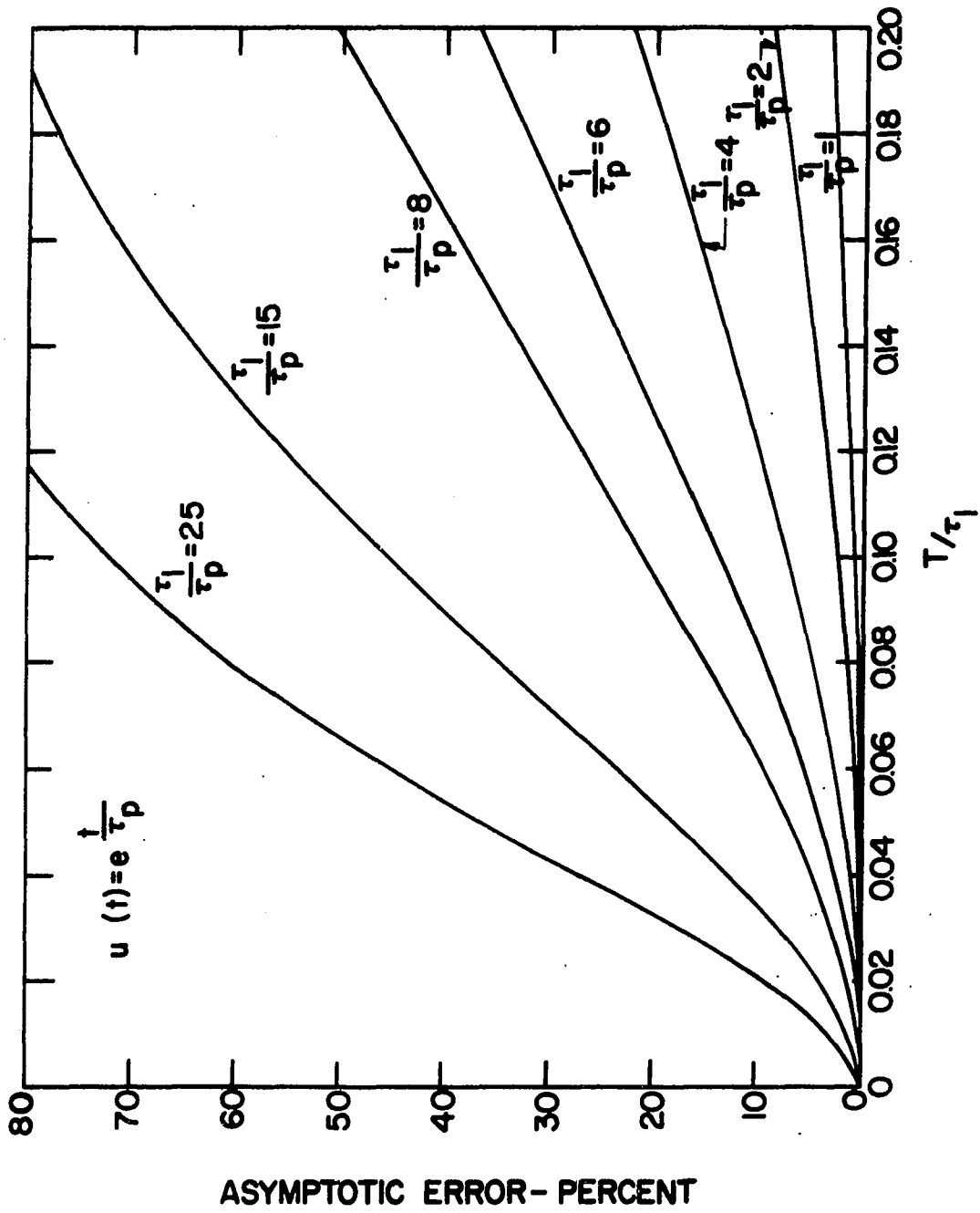


Figure 11. Approximation errors for an inaccessible output state of a unit block with a positive exponential input. Range 2

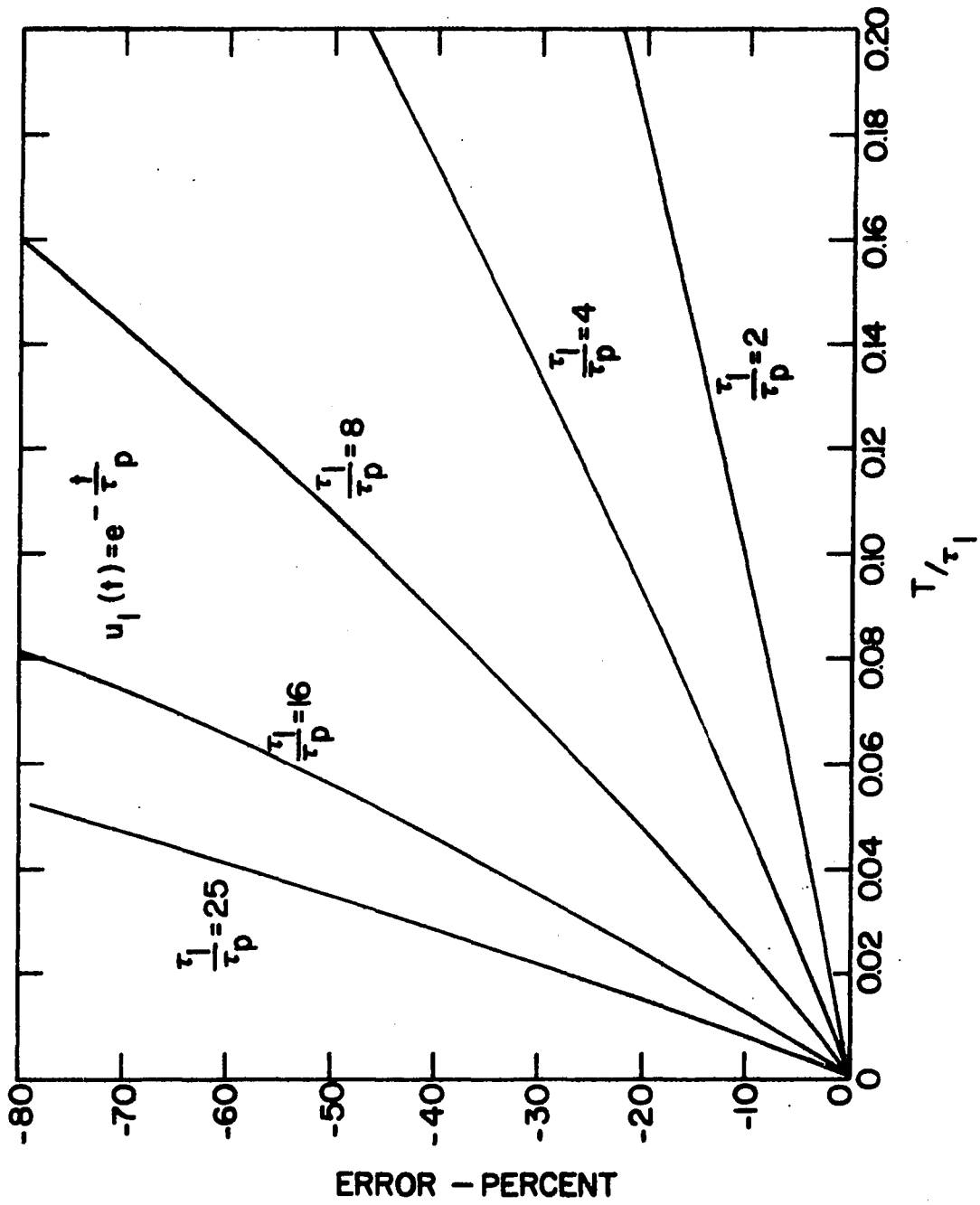


general way the error at early sample periods prior to reaching the asymptotic error. However, the comparison of the accessible and inaccessible output states may prove useful, and it is true that the error is always smaller than the asymptotic value in the earlier sample periods.

d. $u_1(t) = e^{-t/\tau_p}$ The unit step followed by an exponentially decreasing decay has characteristics quite similar to that of the positive exponential. Two characteristics are different. First, the error is negative. The decay makes the approximate solution for the output state have an input that is always equal to the exact input at the sample instant, but at all other times the input is greater. From the error definition of Equation 29, the error is negative. Second, an interesting result from this input is that the error is constant from the very first sample for the inaccessible state. The error, then, does not have to be called an asymptotic error since it is constant as a function of time. The curves for two ranges of T/τ_1 for the inaccessible case are shown in Figures 12 and 13. The results for the accessible case did not reduce to conditions that could be meaningfully displayed on a graph. At the first sample, the error was the same as that for the inaccessible case. After that, the error decreased continually for the twenty samples simulated on the computer. For this type of input, then, the inaccessible state is the only one included here for use.

Figure 12. Approximation errors for an inaccessible output state of a unit block with a unit step and negative exponential decay as an input. Range 1

Figure 13. Approximation errors for an inaccessible output state of a unit block with a unit step and negative exponential decay as an input. Range 2



C. Nonlinear, Time-varying Systems

The previous discussion has been limited to linear, time invariant processes. Unfortunately for the control engineer these characteristics seldom exist. If a linear approximation is used to describe a process that is not linear or time stationary, the major question is the validity of the approximation.

Considering Equation 2 again, the transition matrix is now a function of time and the initial time, t_0 . The general form would be $\Phi(t, t_0)$ instead of that obtained in the linear case $\Phi(t - t_0)$. Even though $\Phi(t, t_0)$ can also be expressed as an exponential as in the time-invariant system, the result is not nearly as satisfactory. There results no formula for $\Phi(t, t_0)$, although Tou (19) indicates that the transition matrix can be expressed as an infinite series of successive integrals. This is not a convenient form with which to work, and general procedures to derive the transition matrix apparently have not yet been obtained.

A non-linearity found in many processes shows up as a product of two of the state variables in the set of first order differential equations describing the plant. Solutions for values of some of the states are needed before all equations can be solved. A simultaneous matrix solution can only be obtained if some iterative technique is used that converges

to the correct values for the states. There is obvious computing time disadvantages of an iterative procedure for a real-time shared digital computer for system control.

There is a type of plant that can be described by a set of first order differential equations which, in matrix form, can be reduced in order and thus simplified. In general, this system is one that has parts of the system separated in space from other parts. In a continuous chemical plant the solution may pass through one tank with a catalyst which will cause a certain reaction to take place. When the solution leaves that tank and proceeds to the next step the reaction will stop because of absence of the catalyst. Mathematically this part of the system can be described by an independent sub-set of the set of equations describing the complete plant. The sub-set can be solved first and the results inserted into the rest of the equations. An example considered in Section IV uses a nuclear reactor as a source of neutrons to activate a radioisotope. No more radioactive isotopes are produced when the sample is removed from the reactor environment. Similarly, a mass isotope separator is used to separate the sample stream. The behavior of the separator and its controls have no effect on the production of the radioactive nuclides in the reactor. These, then, are independent sets of equations and should be able to be solved independently of the complete set.

The advantage of uncoupling or reducing the order of the

set of equations is that one of the states involved in a product of state variables may be in an independent sub-set of the equations. As a consequence, the state can be determined and act as a constant, and the non-linearity is removed. The tool is convenient for use on such non-linear equations.

The independent sub-sets of the complete set are easily recognized when the equations are put in matrix form. If a $q \times q$ block of elements are found in the coefficient matrix with all other elements in the q rows being zero, then these q equations are independent of the other equations in the matrix. One caution is that the driving functions must be checked to see that no states or controls from outside the q rows are encountered. Since the set of first order differential equations describing the system can be placed in any sequence to make up the matrix, the best combination of zero elements in the reduction of the order of the matrix can be obtained.

IV. EXPERIMENTAL IMPLEMENTATION

The adaptive sampling technique using state variable prediction for control has been used in the design of a control system for an experiment in a nuclear reactor. The purpose of the experiment is to investigate the decay schemes of radioisotopes continuously produced and removed from the reactor at a rate approximately equal to the half life of the particular radioisotope. The effect is to produce a radioisotope with an infinite lifetime. The purpose of the control system is to maintain the rate of arrival of the radioactive atoms equal to the rate of decay from the isotope target.

A. Description of Process System

A schematic representation of the system is shown in Figure 14. The nuclear reactor core provides a source of neutrons when the reactor is operating. These neutrons are in close association with a sample in a nearby experimental facility and thus turn a certain portion of the atoms into radioactive atoms by neutron capture. The solid sample is contained in a chamber that is at a high vacuum and is vaporized at a controlled rate by a heater. The vapor flows out of the chamber in the reactor through a tube approximately one inch in diameter and twelve feet long. An ionization

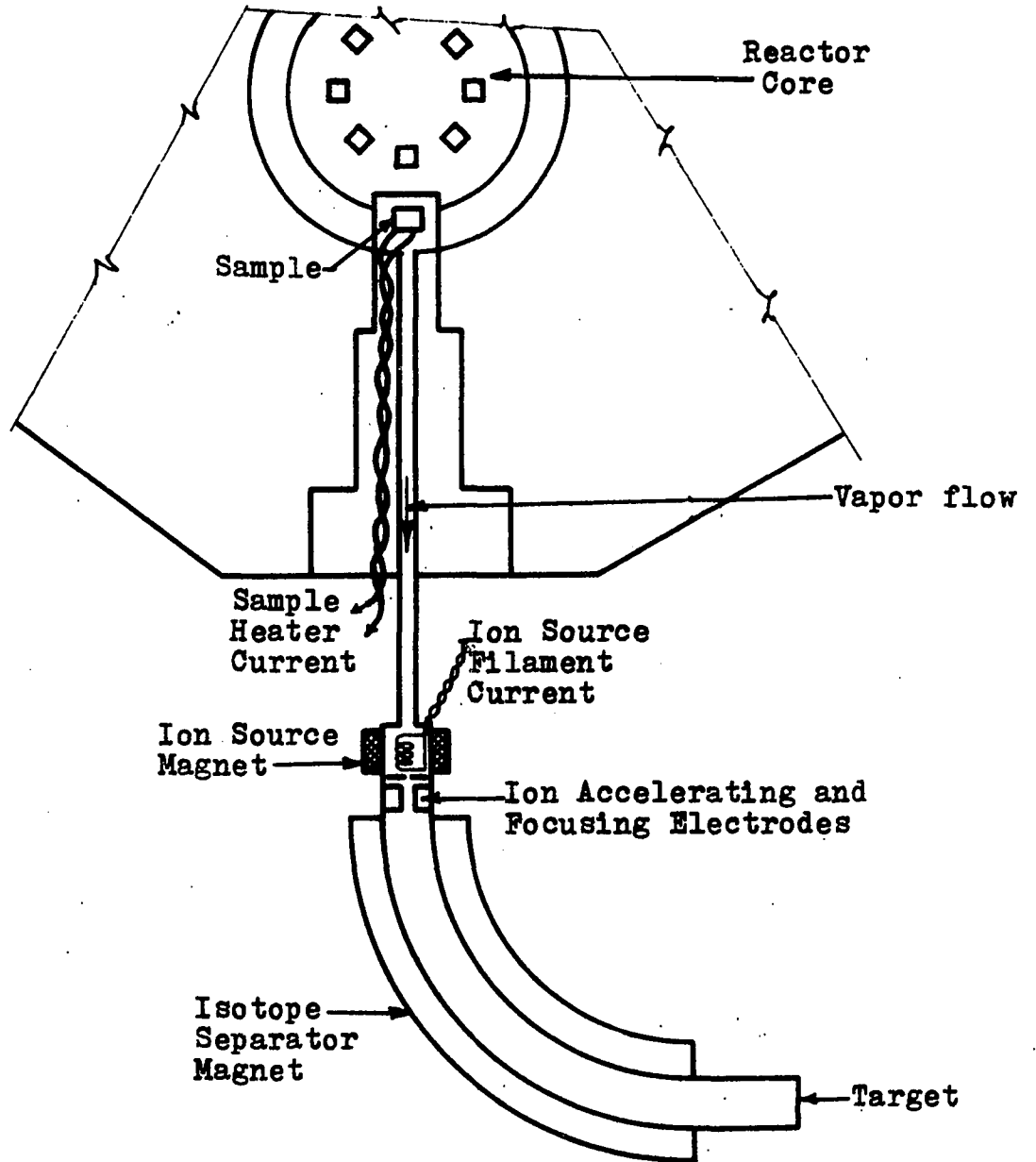


Figure 14. Schematic representation of continuous mass isotope separation of a radioactive sample from a nuclear reactor

source for a mass isotope separator is located at the end of this transfer line. The ion source ionizes the sample vapor and accelerates the resulting ions through a constant potential into the magnetic field of the separator. The separator allows isotopes with different masses to be collected at different physical locations in the plane of the target at the receiving end. At this point the physicist may examine the radioisotopes that have been produced with the appropriate physical tools.

The sample is usually non-radioactive when inserted into the reactor. The buildup of radioactivity depends on the time history of the neutron flux in the reactor, the neutron capture cross section of the atoms and the half life or decay constant of the radioactive nuclides. The vapor from the heated sample will gradually build a pressure that will cause other vaporized atoms to be transported down the line and into the lower pressure area of the ion source and mass isotope separator. The vapor enters a plasma in the ion source that is sustained there by a filamentary heating element, a magnetic field and appropriate element potentials. The vapor becomes ionized when encountering the high temperature of the plasma. A small opening at the end of the ion source, beyond which are located appropriate extracting, accelerating and focusing lens potentials, allows continuous extraction and acceleration of a portion of the ionized radioactive sample. The ions are

accelerated into the magnetic field of the mass isotope separator, and the curvature of the beam along its flight path in the field depends on the mass of the ions. The parent atom normally captures one neutron to form the radioactive daughter atom just one mass unit heavier. The parent and daughter atoms can be separated sufficiently in space to allow separate manipulation by the experimentalist. This action is similar to that in a mass spectrometer used to identify different atomic masses in analytical measurements, except that the mass isotope separator provides a sufficient quantity of atoms to allow physical or chemical experiments. A simplified word block diagram shown in Figure 15 gives a reasonable flow diagram of the interactions that take place in the process.

B. Derivation of Mathematical Model

The process system naturally divides into three parts for studying its mathematical character: the first is forming of radioactive atoms in the sample; the second is producing vapor from the solid sample and transporting the vapor to the inlet of the ion source of the mass isotope separator; the third is converting the non-ionized sample to an ionized form in the ion source and accelerating it through the separator magnetic field to a target. The first objective will be to provide a set of first order differential equations that

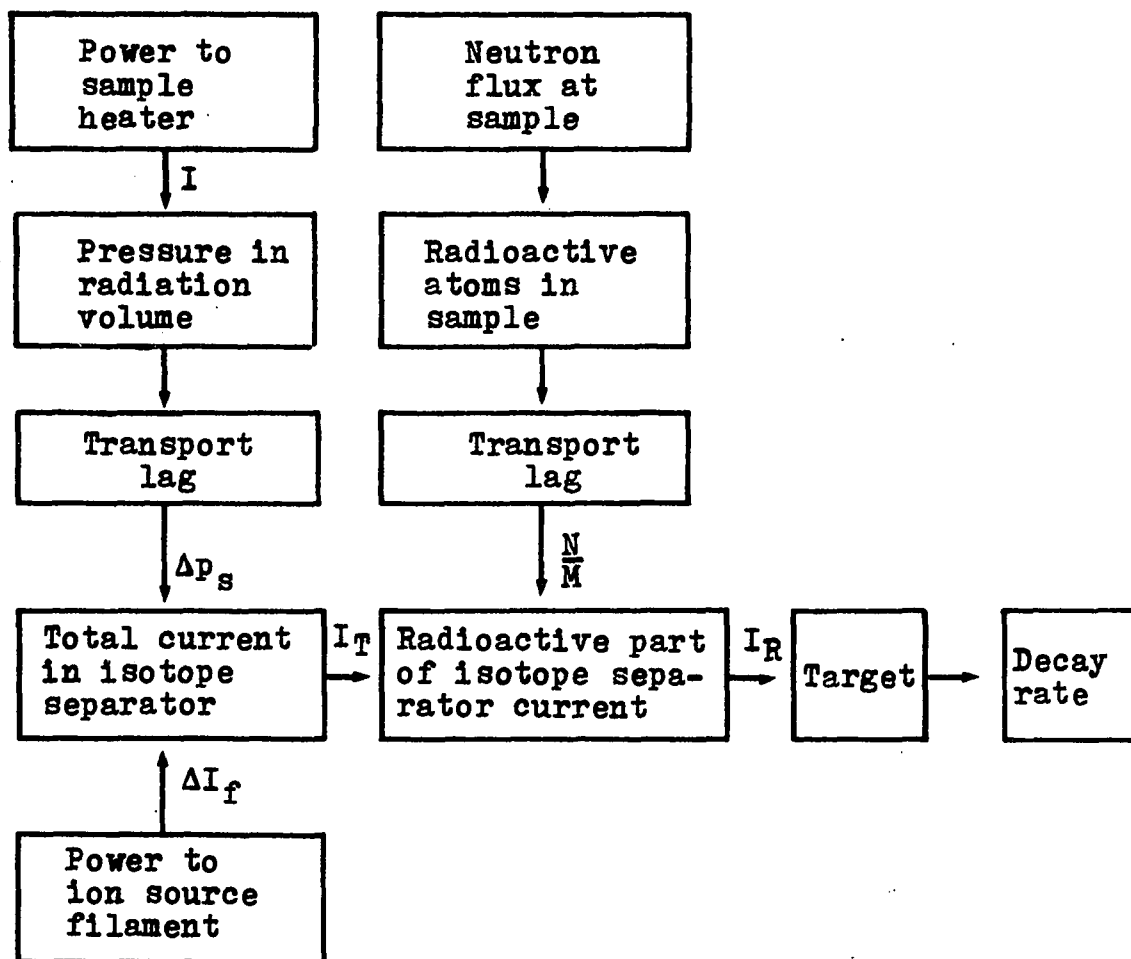


Figure 15. Word flow block diagram of important variables in the experiment

adequately describe the complete process system and the interactions between the variables.

1. Dynamics of sample radioactivity

The differential equations that describe the behavior of a sample in neutron flux are well worked out in the literature (8). The two equations that describe the process for this system are

$$\frac{dN(t)}{dt} = -\lambda N(t) + \sigma M(t)\phi(t) - \frac{N(t) \omega(t)}{N(t) + M(t)} \quad (37)$$

$$\frac{dM(t)}{dt} = -\sigma M(t)\phi(t) - \frac{M(t) \omega(t)}{N(t) + M(t)} \quad (38)$$

where $N(t)$ = number of radioactive atoms at any time,

$M(t)$ = number of parent atoms at any time,

$\phi(t)$ = neutron flux, neutrons/cm²-sec,

σ = neutron capture cross section of the sample, cm²,

λ = decay constant of the sample, sec⁻¹,

t = time, secs, and

$\omega(t)$ = flow of vaporized atoms, atoms/sec.

In Equation 37 the first term on the right is the rate of disappearance of radioactive atoms by decay, the second term is the rate of appearance of new radioactive atoms from capture of neutrons, and the third term is the rate of disappearance of radioactive atoms due to vaporizing and transport-

ing away the solid sample. In Equation 38 the first term is the rate of disappearance of the parent atoms due to the forming of radioactive atoms, and the second term is the rate of disappearance due to transporting away the vaporized sample.

Several approximations for these equations are appropriate when the conditions of the irradiations and the particular samples used in this system are considered. It is expected that a sample will seldom be smaller than 100 grams which is approximately 10^{25} atoms of the parent. The maximum vaporization rate that can be tolerated as an input to the mass isotope separator is approximately 10^{15} atoms/second. Of this total vaporization rate the number that will be radioactive is no greater than 10^9 atoms/second for the half lives, neutron flux and sample cross sections involved. Thus, the ratio N/M is no greater than 10^{-6} . In Equation 38 both terms are negligible compared to the other time constants in the system. Thus $M(t)$ is no longer a function of time but rather a constant equal to the total sample. In the case of a sample that is very small or a combination of a very small sample and a long irradiation time, this approximation is no longer true, and the second differential equation must be considered to give a complete description of the system.

In Equation 37 the rate of change of the number of radioactive atoms in the sample due to vaporization of the radioactive portion compared to the total radioactive atoms present

in the entire sample can similarly be shown to be negligible. The resulting differential equation that describes the dynamic character of the radioactivity in a reasonable sized solid sample in the reactor is

$$\frac{dN(t)}{dt} = -\lambda N(t) + \sigma M \phi(t) \quad (39)$$

where M = the total number of atoms in the solid sample. The useful number that can be derived from the solution of this equation is the ratio N/M since it is the portion of the total vapor that is radioactive as it is vaporized from the solid sample.

The variation of the ratio N/M by the time the vapor enters the ion source is the truly useful quantity, and this ratio can be modified by the transport characteristics of the vapor down the transport line and the decay of radioactive atoms occurring after the sample atoms have left the neutron flux. From the transport characteristics developed in the next section a modification of the ratio is given by another differential equation in R , where R is the ratio of radioactive to parent atoms at the time the vaporized sample enters the ion source. This differential equation is

$$\frac{dR(t)}{dt} = -\frac{1}{\tau_{12}} R(t) + \frac{e^{-\lambda\tau_d}}{\tau_{12}} \frac{N(t - \tau_d)}{M} \quad (40)$$

where τ_{12} = the response time of pressure at the ion source to a change in pressure at radiation volume, sec

τ_d = transport lag from the radiation volume to the ion source, sec, and

R = ratio of number of radioactive to parent atoms at the ion source.

The term, $e^{-\lambda\tau_d}$, is the exponential decay of the radioactive portion after leaving the reactor. This transport lag is a function of the molecular weight of the sample and the rate at which the sample is being vaporized. The molecular weight, of course, is constant for a given sample except for the radioactive atoms which are one mass unit heavier than the parent atoms. The rate of flow varies no more than 2 to 1, since the ion source for the isotope separator will not operate over a greater range of flow variation. The result is that this term is nearly a constant for a given sample.

2. Dynamics of sample transport

The irradiation of a solid sample, and then depending upon its vapor pressure to transport it to the ion source, requires that the rest of the transport line through which the vapor is passed be above the temperature that would allow plating out at the sample vapor pressure. The loop from the irradiation chamber to the inlet of the ion source will be kept at a constant temperature above that necessary for the control range in vaporizing the sample. Typical operating

temperatures range from 300°C to 675°C to allow the proper vaporization rate for some of the rare earth chlorides and metals expected to be used. The control range of the temperature is from 20°C to 30°C to provide the proper range of flow rates to the ion source for a given sample. This range of operation vaporizes from 7×10^{14} to 1.5×10^{15} atoms/sec typically for the size samples expected. Table 1 lists information for some specific compounds to be used. The sensitivity of vaporization to temperature, the minimum operating temperature and the range of operation necessary to provide the desired atoms per second at the ion source are listed.

The variation of the vaporization rate of a sample with temperature is exponential. However, over the small temperature range of operation, the approximation that it is incrementally linear is very good as can be seen in Figure 16, showing the calculated vaporization rate versus temperature for $GdCl_3$. The range of operation required in the ion source of the mass isotope separator is indicated in the figure.

The sample transport dynamics divide naturally into two parts, the vaporization of the sample from the solid and the transport of the vapor to the ion source. The rate of vaporization of the sample is controlled by the rate at which power is put into a heater surrounding the sample being irradiated in the reactor. There is a lag between applying the power to the heater and the transfer of the heat into the sample which

Table 1. Vaporization characteristics of sample compounds

Compound	T_{sm} , Minimum operating temperature (°C)	K_g , Incremental vaporization sensitivity (atoms/°C)	ΔT_{sm} , Operating temperature range (°C)
YCl ₃	501	2.45×10^{13}	12
NdCl ₃	672	2.40×10^{13}	13
SmCl ₂	431	1.80×10^{13}	30
EuCl ₃	487	2.55×10^{13}	21
GdCl ₃	612	2.55×10^{13}	21
DyCl ₃	613	2.90×10^{13}	18
ErCl ₃	563	2.20×10^{13}	25
Y ₆ Cl ₃	666	2.50×10^{13}	22
LuCl ₃	660	3.00×10^{13}	18
Eu (metal)	317	2.50×10^{13}	22

raises its temperature. An ideal example was solved for heat transfer in the case of an infinitely long cylinder of Europium metal, that is, assuming no heat flow along the cylinder. An initial equilibrium temperature was established at the cylinder wall and all temperatures within the cylinder were assumed to come to this same temperature. The surface of the cylinder was then given a step in temperature. The plot in Figure 17 shows the change of temperature within the cylinder as a function of cylinder radius and time for any

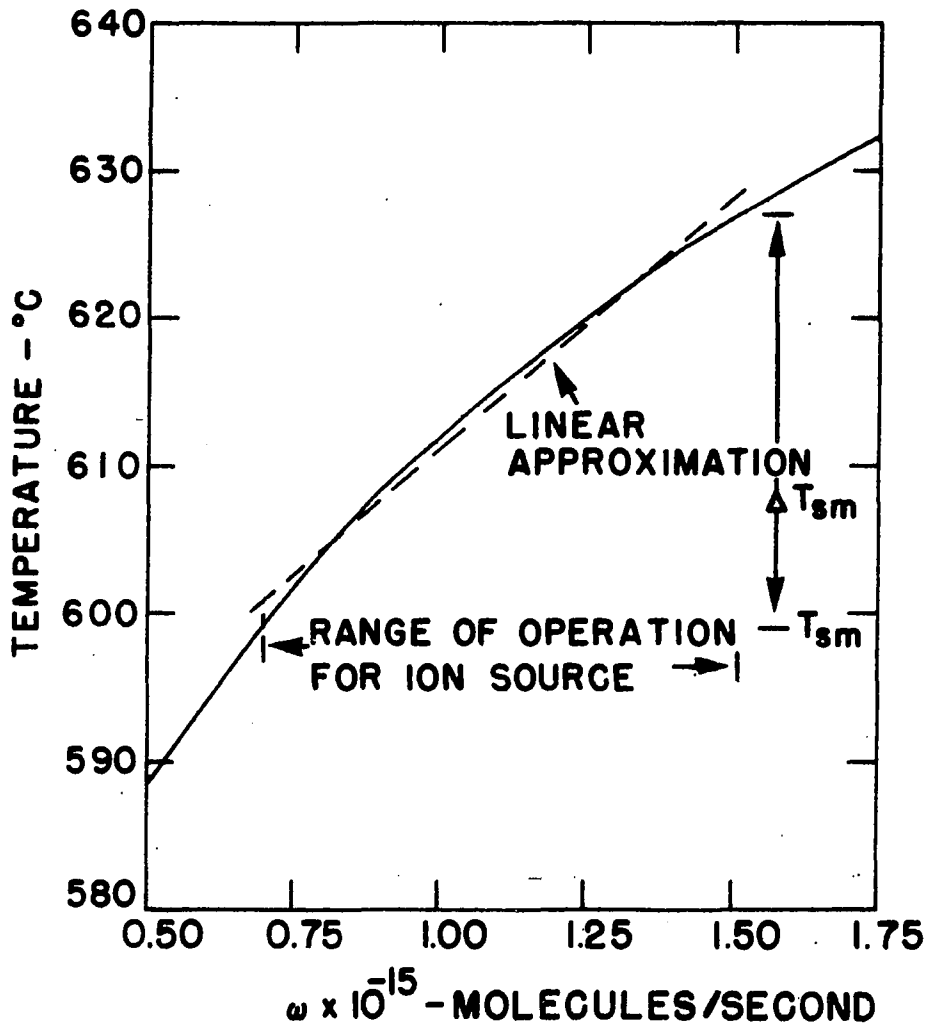


Figure 16. Vaporization of $GdCl_3$ as a function of temperature

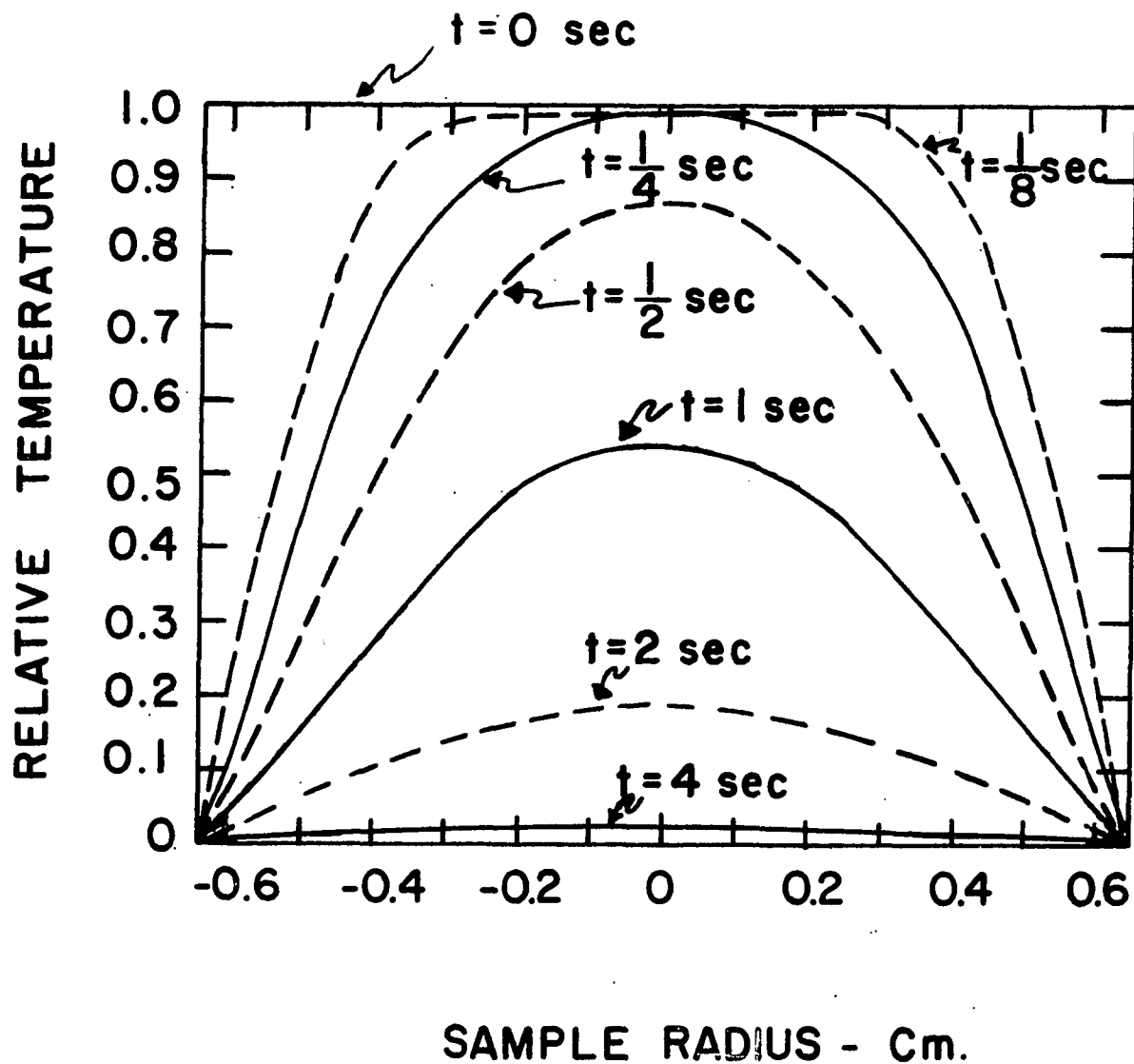


Figure 17. Normalized time-temperature characteristics of Europium metal for an incremental change in temperatures

material with the diffusivity of Europium metal. Little exact information is available on the diffusivity of the rare earth chlorides. However, in general their diffusivities are reduced about a factor of 20 from that of the metals. Thus, they would have a similar shape, but a factor of 20 times each of the time values shown. It would be desirable to build a sample heater arrangement to investigate these properties for proposed samples. This has been done for the flow system as will be explained.

If it is assumed that the vaporization will occur from the top millimeter or so of surface, i.e., that the vaporization is mainly a surface phenomenon, then it appears that a first order time lag will describe the vaporization as a function of sample heater power. In differential equation form this becomes

$$\frac{d\Delta T_s(t)}{dt} = -\frac{1}{\tau_6} \Delta T_s(t) + \frac{K_6}{\tau_6} \Delta P_H(t) \quad (41)$$

where ΔT_s = incremental variation of sample temperature at operating temperature levels, °C,

ΔP_H = incremental variation of sample heater power at operating power levels, watts,

τ_6 = time constant of the temperature change from a change in heater power, sec, and

K_6 = effect of sample heater power on sample temperature, °C/watt.

In order to relate ΔP_H to the measurable parameter ΔI_H , the

incremental heater current change, the heater resistance in the operating range is assumed to remain constant at R_H . Then

$$\Delta P_H(t) = R_H \Delta I_H^2(t) + 2I_{Hm} R_H \Delta I_H(t) \quad (42)$$

where I_{Hm} = minimum operating heater current, amps, and

R_H = operating resistance of heater, ohms.

The transport of the sample from the point at which it is a vapor into the transport line and to the ion source inlet is complicated. The pressures and the rates of flow involved cover a region that is partially laminar flow and partially flow by molecular diffusion. Thus, it is difficult to calculate and provide an accurate mathematical model of this part of the system. To provide a reasonable mathematical model, an experimental arrangement was set up using gas flow instead of vapor to study the dynamics. The results indicate the transport lag is in the range from approximately 0.3 seconds to 1.5 seconds, and the first order time constant which fairly well represents the system behavior ranges from approximately 0.5 seconds to 1.5 seconds, both numbers varying with the molecular weight of the gas. This results in a differential equation describing the dynamics of the flow as

$$\frac{d\Delta p_s(t)}{dt} = -\frac{1}{\tau_{12}} \Delta p_s(t) + \frac{K_{12}}{\tau_{12}} \Delta T_s(t - \tau_d) \quad (43)$$

- where Δp_s = incremental pressure at the ion source inlet, microns,
- ΔT_s = incremental temperature variation of sample at operating levels, °C,
- τ_{12} = the time constant of response of the pressure at the ion source for a change of temperature of the sample, sec,
- K_{12} = effect of sample temperature on pressure at the ion source, micron/°C, and
- τ_d = transport lag, sec.

3. Dynamics of mass isotope separator

The ion source of the isotope separator has five variables that effect the total isotope current received at the target of the separator. These variables are ion source filament current, ion source magnet current, focus voltage, extraction voltage, and the rate at which sample is being inserted in vapor or gas form into the source. One of these variables, the sample flow rate, is already varying according to the sample vapor created back in the reactor experiment location. The speed with which the flow rate changes is quite slow compared to the speed of the other variable responses in the isotope separator. Of these variables, experiments show that the ion source filament current varies the total isotope separator current over a wider range than any of the other variables without affecting other system conditions.

A family of curves plotting total isotope separator current versus ion source filament current for various con-

stant values of sample flow into the ion source (in terms of pressure) allows evaluation of the constants K_1 and K_2 which relate filament current and pressure inlet to isotope total current flow in the separator. This family of curves shown in Figure 18 can be used with the same analytical techniques commonly used with curves of triode vacuum tubes. The desirability of incremental variables up to this point then becomes apparent. The incremental inputs Δp_s and ΔI_f can be used in direct computation for an incremental change in total isotope separator current ΔI_t . Thus,

$$\Delta I_t(t) = K_1 \Delta I_f(t) + K_2 p_s(t) \quad (44)$$

where $K_1 = \left(\frac{\partial I_t}{\partial I_f} \right)_{p_s} = \text{constant},$

$$K_2 = \left(\frac{\partial I_t}{\partial p_s} \right)_{I_f} = \text{constant},$$

ΔI_f = incremental ion source filament current, amps,
and

ΔI_t = incremental isotope separator total current, amps,

and the constants K_1 and K_2 are determined from the family of curves in Figure 18. For the range of operation acceptable to the ion source, the approximation that K_1 and K_2 are constant instead of variable is a good one. It should be noted that there is a response time of about one-half second for the effect on isotope separator current of a change in ion source filament current. This is considered negligible compared to other time constants in the system and is thus disregarded.

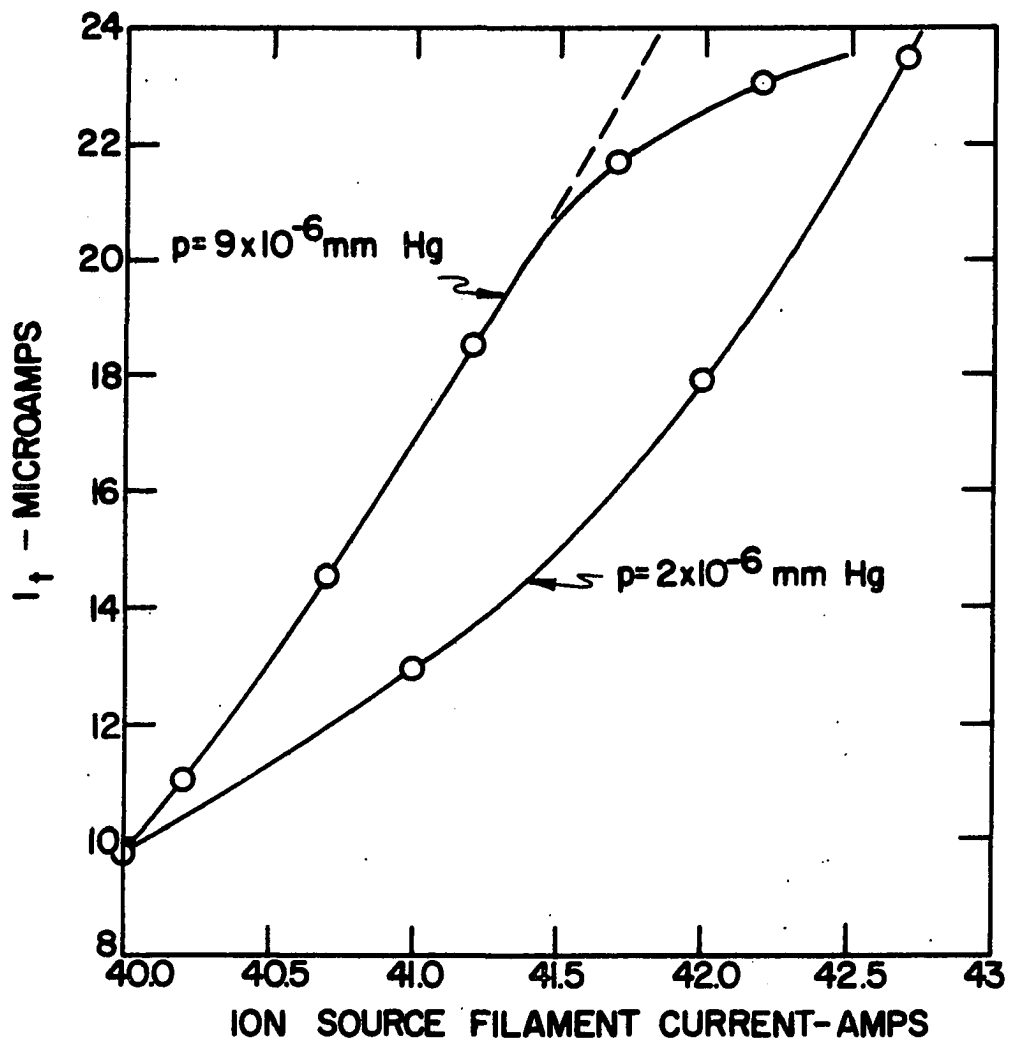


Figure 18. Experimental curves from a mass isotope separator showing relation among variables. Dotted line indicates expected normal curve

At this point in the development of the system equations, a departure from incremental variable descriptions is desirable since the final equation will determine how many atoms of the total isotope separator beam are radioactive and the number of these that are decaying each second. Thus, the total beam current is

$$I_t(t) = I_{tm} + \Delta I_t(t) \quad (45)$$

where I_t = total isotope separator current, amps

I_{tm} = minimum desired operating isotope separator current, amps.

In terms of the two variables already described, then

$$I_t(t) = I_{tm} + K_1 \Delta I_f(t) + K_2 \Delta p_s(t) \quad (46)$$

which completes the dynamics for the mass isotope separator.

4. Combined dynamics at the target

The total number of atoms per second of the sample arriving at the target of the mass isotope separator has been determined, and the ratio of radioactive to total atoms in this beam as a function of time has also been described. The pertinent information is the product of these two since it is desired to control the number of radioactive atoms per second arriving at the target. Thus

$$I_R(t) = R(t) [I_{tm} + K_1 \Delta I_f(t) + K_2 \Delta p_s(t)] \quad (47)$$

where I_R = radioactive atoms/sec arriving at target.

If the number of radioactive atoms on the target at any one time is N_T , then the differential equation describing the rate of change of N_T with time is just the rate at which they are arriving on the target less the rate at which they are decaying. Thus,

$$\frac{dN_T(t)}{dt} = K_{10}I_R(t) - \lambda N_T \quad (48)$$

where $K_{10} = 6.3 \times 10^{18}$ atoms/amp.

Finally, the desired output of the system is an average decay rate which is just the number of radioactive atoms on the target at any time times the decay constant. Thus,

$$D_a(t) = \lambda N_T(t) \quad (49)$$

where D_a = decay rate of the radioactive atoms from the target, disintegrations/second.

Making the substitutions of D_a into the differential equations for N_T results in the following differential equation for the decay rate as a function of the other variables.

$$\frac{dD_a(t)}{dt} = -\lambda D_a(t) + \lambda K_{10}R(t) [I_{tm} + K_1 \Delta I_f(t) + K_2 \Delta p_s(t)] \quad (50)$$

This completes the set of differential equations which will be used to mathematically approximate the system. The equations

are listed here again for easy reference.

$$\frac{dN(t)}{dt} = -\lambda N(t) + \sigma M_T \phi(t) \quad (39)$$

$$\frac{dR(t)}{dt} = -\frac{1}{\tau_{12}} R(t) + \frac{e^{-\lambda \tau_d}}{\tau_{12}} \frac{N(t - \tau_d)}{M} \quad (40)$$

$$\frac{d\Delta T_s(t)}{dt} = -\frac{1}{\tau_6} \Delta T_s(t) + \frac{K_6}{\tau_6} \Delta P_H(t) \quad (41)$$

$$\frac{d\Delta p_s(t)}{dt} = -\frac{1}{\tau_{12}} \Delta p_s(t) + \frac{K_{12}}{\tau_{12}} \Delta T_s(t - \tau_d) \quad (43)$$

$$\frac{dD_a(t)}{dt} = -\lambda D_a(t) + \lambda K_{10} R(t) \left[I_{tm} + K_1 \Delta I_f(t) + K_2 \Delta p_s(t) \right] \quad (50)$$

where the following interrelations are noted:

$$I_t(t) = I_{tm} + K_1 \Delta I_f(t) + K_2 \Delta p_s(t) \quad (46)$$

$$\Delta I_t(t) = K_1 \Delta I_f(t) + K_2 \Delta p_s(t) \quad (44)$$

$$\Delta P_H(t) = R_H \Delta I_H^2(t) + 2I_{Hm} R_H \Delta I_H(t) \quad (42)$$

These differential equations can also be represented in block diagram form using Laplace transforms. This is shown in Figure 19. Due to the nonlinearities present, particularly the product, $R(t)I_t(t)$, of two time varying functions, it is difficult to design a control system directly using this form of the block diagram. Nevertheless, the process described in

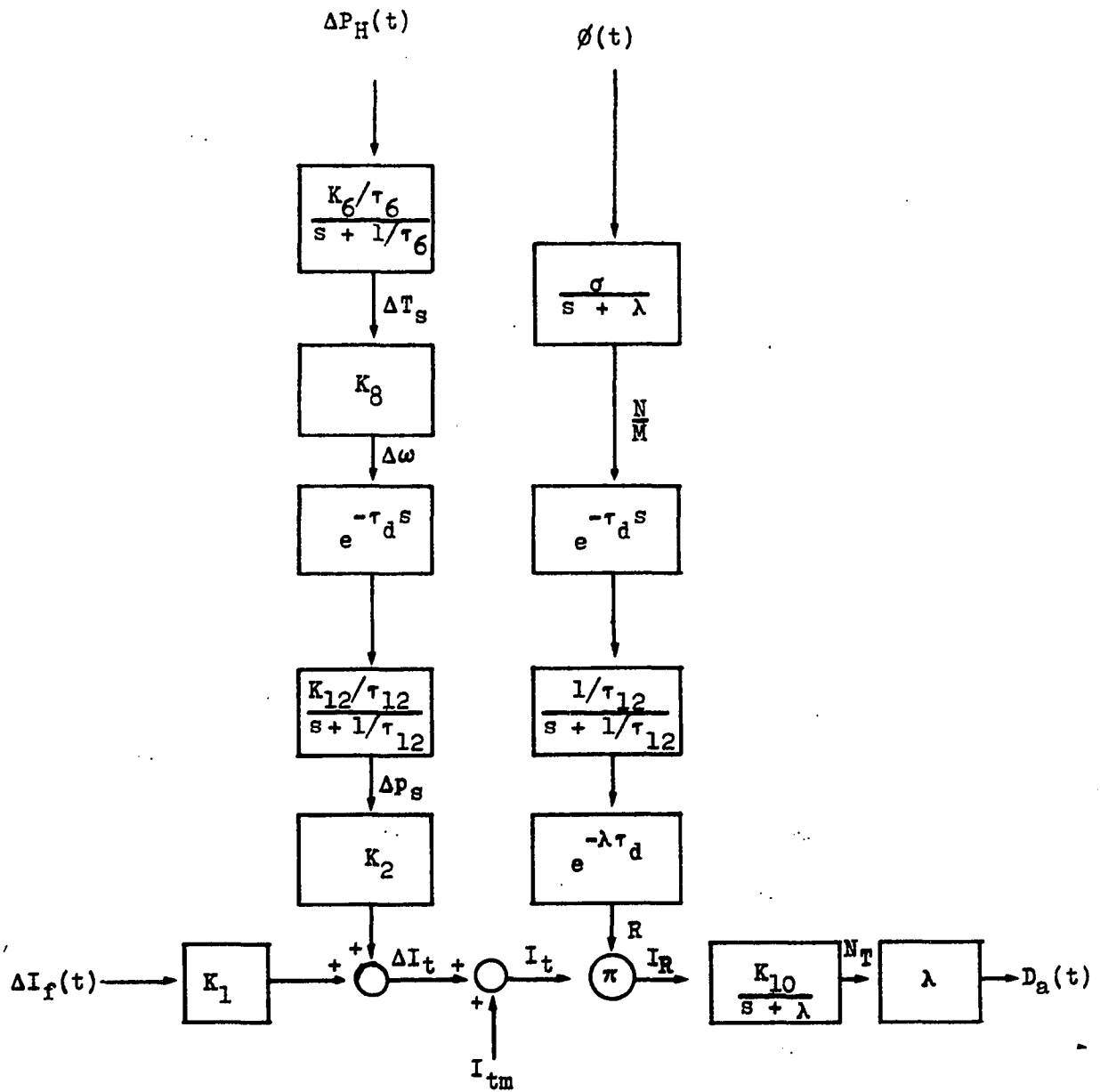


Figure 19. Block diagram of experimental system dynamics

this form is useful for certain control concepts.

C. Solution for System Equations

The set of differential equations derived to describe the process has both nonlinear relations and transport lags between some of the variables. Some of the individual equations, however, are either linear or incrementally linear over the range of operation. These equations are those that occur first in the space separation of this type of process and thus are unperturbed by variables occurring further along in the process. The process of generating the mathematical model of this system has shown that some of the equations can be solved independently of the others. Nevertheless, in the interest of generality, the equations will be investigated as a set of equations to show how the sequential solutions evolve.

The set of differential equations developed in Section B can be placed in matrix form which tends to make certain mathematical manipulations easier as well as making it easier to see such things as nonlinearities and time-varying coefficients. The form of the matrix necessary to represent this system is

$$\bar{x}(t) = A(\bar{x}, t)\bar{x}(t) + B(\bar{x}, t)\bar{x}(t - \tau_d) + \bar{u}(t) \quad (51)$$

where $x_1(t)$ is the typical state variable at time t , A and B

are time-varying nonlinear coefficient matrices, and $\bar{u}(t)$ contains the time-varying driving functions. Using the variable designations already adopted, the form of the fifth order system describing the plant in matrix form is

$$\begin{pmatrix} \dot{N}(t) \\ \Delta \dot{T}_s(t) \\ \Delta \dot{p}_s(t) \\ \dot{R}(t) \\ \dot{D}_a(t) \end{pmatrix} = \begin{pmatrix} -\lambda & 0 & 0 & 0 & 0 \\ 0 & -\frac{1}{\tau_6} & 0 & 0 & 0 \\ 0 & 0 & -\frac{1}{\tau_{12}} & 0 & 0 \\ 0 & 0 & 0 & -\frac{1}{\tau_{12}} & 0 \\ 0 & 0 & [\lambda K_{10} K_{12} R(t)] & [\lambda K_{10} (I_{tm} + K_1 \Delta I_f(t))] & -\lambda \end{pmatrix} \begin{pmatrix} N(t) \\ \Delta T_s(t) \\ \Delta p_s(t) \\ R(t) \\ D_a(t) \end{pmatrix} \quad (52)$$

$$+ \begin{pmatrix} 0 & 0 & 0 & 0 & 0 \\ 0 & 0 & 0 & 0 & 0 \\ 0 & \frac{K_{12}}{\tau_{12}} & 0 & 0 & 0 \\ \frac{e^{-\lambda \tau_d}}{M \tau_{12}} & 0 & 0 & 0 & 0 \\ 0 & 0 & 0 & 0 & 0 \end{pmatrix} \begin{pmatrix} N(t - \tau_d) \\ \Delta T_s(t - \tau_d) \\ \Delta p_s(t - \tau_d) \\ R(t - \tau_d) \\ D_a(t - \tau_d) \end{pmatrix} + \begin{pmatrix} \sigma M \phi(t) \\ \frac{K_6}{\tau_6} \Delta P_H(t) \\ 0 \\ 0 \\ 0 \end{pmatrix}$$

The element a_{53} shows nonlinearity with two of the state variables multiplied together. The element a_{54} indicates a time-varying coefficient since one of the inputs is multiplied by one of the state variables. The element b_{32} indicates that

a transport lag is involved with the determination of one of the state variables. The element b_{41} indicates both transport lag and the time variation of τ_d in determining one of the state variables.

The first two equations in the matrix are not functions of the last three state variables, since there are 2 x 3 blocks of zeros in the upper right hand corner of both the coefficient matrices, A and B. Thus, these two equations can be separated from the other three resulting in the formation of two matrices, a process referred to as uncoupling. The two matrices then are

$$\begin{pmatrix} \dot{N}(t) \\ \Delta \dot{T}_s(t) \end{pmatrix} = \begin{pmatrix} -\lambda & 0 \\ 0 & -\frac{1}{\tau_6} \end{pmatrix} \begin{pmatrix} N(t) \\ \Delta T_s(t) \end{pmatrix} + \begin{pmatrix} \sigma M \phi(t) \\ \frac{K_6}{\tau_6} \Delta P_H(t) \end{pmatrix} \quad (53)$$

and

$$\begin{pmatrix} \Delta \dot{p}_s(t) \\ \dot{R}(t) \\ \dot{D}_a(t) \end{pmatrix} = \begin{pmatrix} -\frac{1}{\tau_{12}} & 0 & 0 \\ 0 & -\frac{1}{\tau_{12}} & 0 \\ [\lambda K_{10} K_{12} R(t)] & [\lambda K_{10} (I_{tm} + K_1 \Delta I_f(t))] & -\lambda \end{pmatrix} \begin{pmatrix} \Delta p_s(t) \\ R(t) \\ D_a(t) \end{pmatrix} + \begin{pmatrix} \frac{K_{12}}{\tau_{12}} \Delta T_s(t - \tau_d) \\ -\lambda \tau_d \\ \frac{e}{M \tau_{12}} N(t - \tau_d) \\ 0 \end{pmatrix} \quad (54)$$

It is necessary to solve the 2 x 2 matrix in Equation 53 first

and then substitute values for $\Delta T_S(t - \tau_d)$ and $N(t - \tau_d)$ into the matrix in Equation 54 as driving functions. This is reasonable since they are now known values not unknown variables.

Further examination, of course, shows that these two resulting matrices can again be broken apart or uncoupled again requiring the solution of one equation and substituting the result into the next before it can be solved. This results in a step by step solution of one equation at a time for this fifth order system of differential equations. The complicating problem is that the solutions of each of the equations becomes more and more complex as the time-varying driving functions accumulate from one equation to the next.

The sequence is as follows:

1. Solve the first two equations for $N(t)$ and $\Delta T_S(t)$ by substituting in the driving functions $\phi(t)$ and $\Delta P_H(t)$ respectively. These are ordinary differential equations which can be solved by any of the usual techniques for these types of equations once the driving function is known.

$$\dot{N}(t) = -\lambda N(t) + \sigma M \phi(t) \quad (55)$$

$$\Delta \dot{T}_S(t) = -\frac{1}{\tau_6} \Delta T_S(t) + \frac{K_6}{\tau_6} \Delta P_H(t) \quad (56)$$

2. Using the solution of $\Delta T_S(t)$, determine $\Delta T_S(t - \tau_d)$ and substitute as a driving function into the third differential equation,

$$\Delta \dot{p}_s(t) = -\frac{1}{\tau_{12}} \Delta p_s(t) + \frac{K_{12}}{\tau_{12}} \Delta T_s(t - \tau_d) \quad (57)$$

3. Using the solution of $N(t)$, determine $N(t - \tau_d)$ and substitute as a driving function into the fourth differential equation,

$$\dot{R}(t) = -\frac{1}{\tau_{12}} R(t) + \frac{e^{-\lambda \tau_d}}{M \tau_{12}} N(t - \tau_d) \quad (58)$$

4. Using the solution of $\Delta p_s(t)$ and $R(t)$ from parts 2 and 3 above, substitute into the last differential equation as driving functions

$$\dot{D}_a(t) = -\lambda D_a(t) + \lambda K_{10} R(t) \left[K_2 \Delta p_s(t) + K_1 \Delta I_f(t) + I_{tm} \right] \quad (59)$$

The solution of the last equation then gives the variation in the decay rate of the radioactive isotope from the target of the mass isotope separator. This decay rate varies with the three inputs $\phi(t)$, $I_H(t)$, and $I_f(t)$ of which the latter two are available for control variation by the control system.

This process is an example of the type discussed in Section III-C. The process is described by a set of nonlinear differential equations with time-varying coefficients. The nature of the process, where an entity starts at one end of the system, passes completely through the system, and then disappears, is such that the nonlinear system can be uncoupled into pieces that in smaller sections behave as a linear system.

D. System Control

The design of the system for this experiment is an optimum control problem similar to that described by Tou (19). The control policy or law for the optimum control system is the sequence of inputs, $\{\bar{m}(i)\}$, $i = 0, 1, 2, \dots, N - 1$, which minimizes the expected value of a performance index subject to Equation 18 for any arbitrary initial state $\bar{x}(t_0)$. The performance index for this experiment is given as

$$I_N = \bar{x}(t_{k+1})_{\text{exact}} - \bar{x}(t_{k+1})_{\text{approx.}} \quad (60)$$

where I_N is the performance index that is to be minimized in N steps of the driving function inputs. The driving functions in this system can bring the performance index to a minimum within each step of the control system so $N = 1$.

The development of the adaptive sampling design method in Section III gave no consideration to the problem of stability. According to Kalman and Bertram (10), stability in a linear system depends only on the transition matrix (Equation 8) of the system. Stability cannot be brought about or destroyed by a particular choice of the initial state or the system input signal. A stationary linear system is stable if and only if every element of the transition matrix tends to zero as N tends to infinity where N is the number of times that the transition matrix is multiplied times itself. For a constant

transition matrix, a stationary linear system is stable if all roots of the characteristic equation of the transition matrix are less than unity. This condition is identical with the result that the poles of the z-transform of the input-output relations of the system must lie within the unit circle. The stationary transition matrix is only obtained where the pattern of the sampling operations repeats in a periodic fashion.

The fifth order set of differential equations that describe this system are a nonlinear set which cannot be analyzed with the elementary stability criterion described above. However, when the system is uncoupled and each equation is solved in sequence there are five linear first order transition matrices. Each of these are of the form, e^{-u} , with the value of u being greater than zero in every case. This means that the scalar transition matrices all have values less than one and, since they are a stationary transition matrix within each mode of operation, the control system is claimed to be stable for any values of cross section and half life of samples in the experiment. With these few comments the stability of the system will be given no further consideration as a part of this development.

1. Multilevel control equations

Two control driving functions are shown for the system in Figure 19. One of the inputs can be used as a course adjust-

ment, making the fine adjustment by the second input a much simpler task. Other objectives also may be realized. The necessity of solving nonlinear differential equations may be eliminated. The error associated with the approximation of the prediction of the output states may be reduced. The matrix form of the fifth order system describing the plant is given in Equation 19. One of the nonlinearities here is indicated by element a_{53} where two state variables $R(t)$ and $\Delta p_s(t)$ are multiplied together. This product is the ratio of radioactive to non-radioactive atoms times the pressure of the vapor at the inlet to the ion source. Since the pressure at the outlet of the ion source in the isotope separator is negligible compared to the ion source inlet pressure, the inlet pressure, Δp_s , is incrementally proportional to flow. The product is incrementally proportional to the number of radioactive atoms flowing into the ion source per second. Since the purpose of the control system is to maintain constant the number of radioactive atoms arriving at the target of the isotope separator, the possibility of making constant the number of radioactive atoms per second flowing into the ion source is quite attractive.

The block diagram of the experimental system dynamics shown in Figure 19 shows an interesting relationship between the product of the two state variables R and Δp_s and the product of the two state variables N/M and ΔT_s . Since N/M and

ΔT_s are both modified by the transport lag and time constant of the transportation of the vapor from the sample chamber to the ion source, their products would be proportional to that of R and Δp_s if the decay of the radioactivity indicated by the term, $e^{-\lambda \tau_d}$, is either constant or negligible. Since the transport lag has been measured experimentally and found to be no greater than 1.5 seconds in the worst case, the minimum half life of 15 seconds makes the decay between the reactor and the ion source negligible. In addition, the transport lag is likely to vary no more than a factor of three for the range of molecular weights in samples to be run in the experiment.

The product $\Delta T_s N/M$ is incrementally proportional to the number of radioactive atoms per second being vaporized from the sample, just as $R \Delta p_s$ is incrementally proportional to the rate of arrival of radioactive atoms in the ion source. Since the control driving function, ΔP_H , varies the number of atoms per second being vaporized from the sample, the first control loop can now be defined. From the measured value of the sample temperature and the calculated value of the number of radioactive atoms in the sample a prediction can be made using the approximation equations developed earlier. The product of the two predicted values can be held nearly constant by changing the value of the sample heater current. In addition to the approximation error for the state variable N/M there is a small but finite time required for the calculations after the

measurement of the state, ΔT_s . This delay can be as small as 10 milliseconds and as large as 500 milliseconds depending on the program and the availability of the computer. Since sample times for control will range from about 5 seconds apart to more than 30 seconds apart, the computational delays will produce small errors.

Since the transport lag from the sample to the ion source is so short compared to the half life of any sample to be used, a good approximation is that

$$R(t) \approx \frac{N(t)}{M} \quad (61)$$

With this approximation the block diagram for the control loop defined in the last paragraph is shown in Figure 20.

The fine control can be defined by examining Equation 59. Using the approximation of Equation 61 and noting that the product of the two state variables is now a constant, the equation becomes

$$\dot{D}_a(t) = -\lambda D_a(t) + \lambda K_{10} \left[C + \frac{N(t)}{M} (K_1 \Delta I_f(t) + I_{tm}) \right] \quad (62)$$

where

$$C = K_2 \Delta p_s(t) \frac{N(t)}{M} \quad (63)$$

Equation 62 can be shown in an equivalent block diagram form in Figure 21. The control of the ion source filament current, ΔI_f , is carried out identically to that of ΔP_H of the first

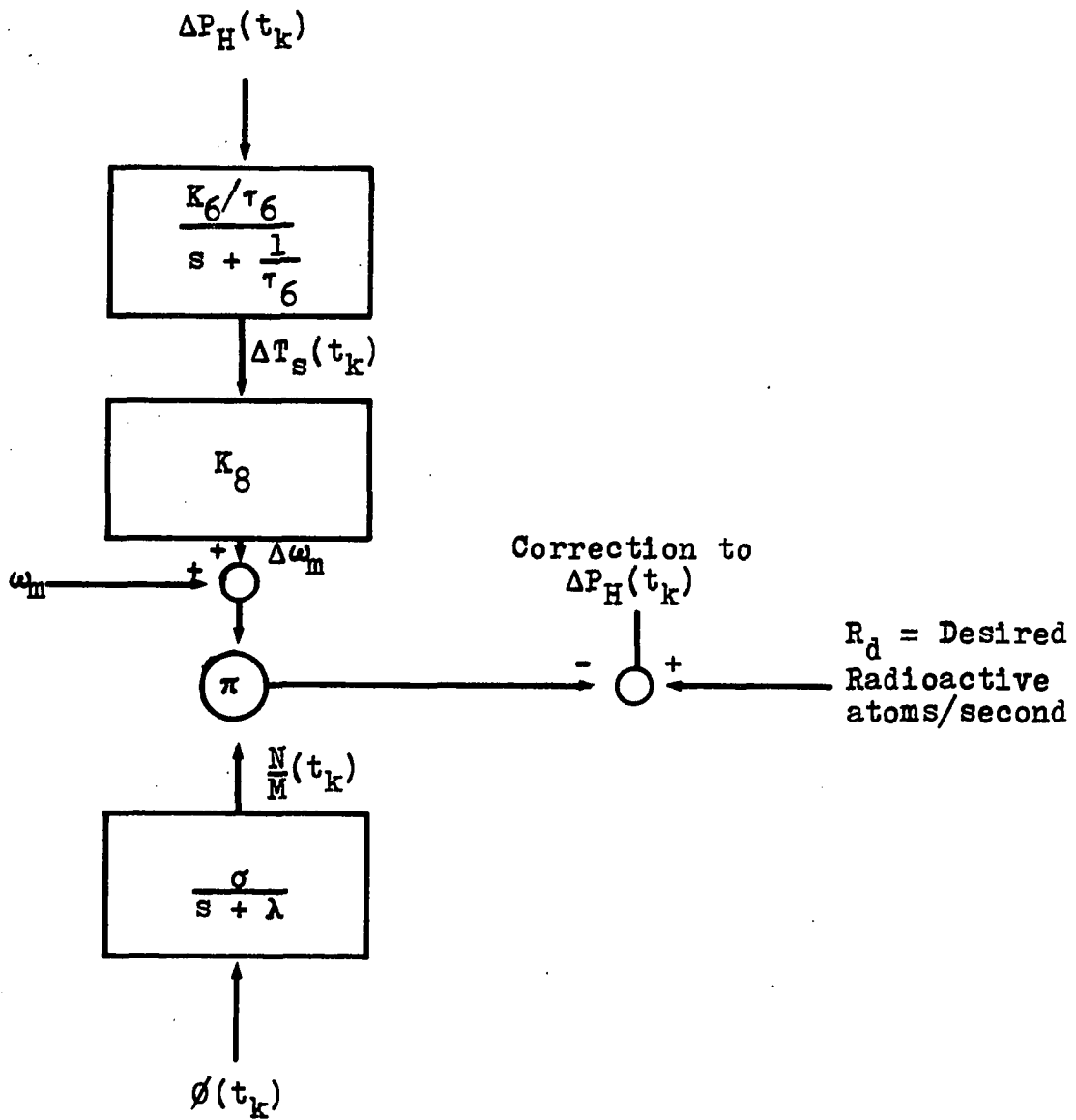


Figure 20. Block diagram of control for sample heater

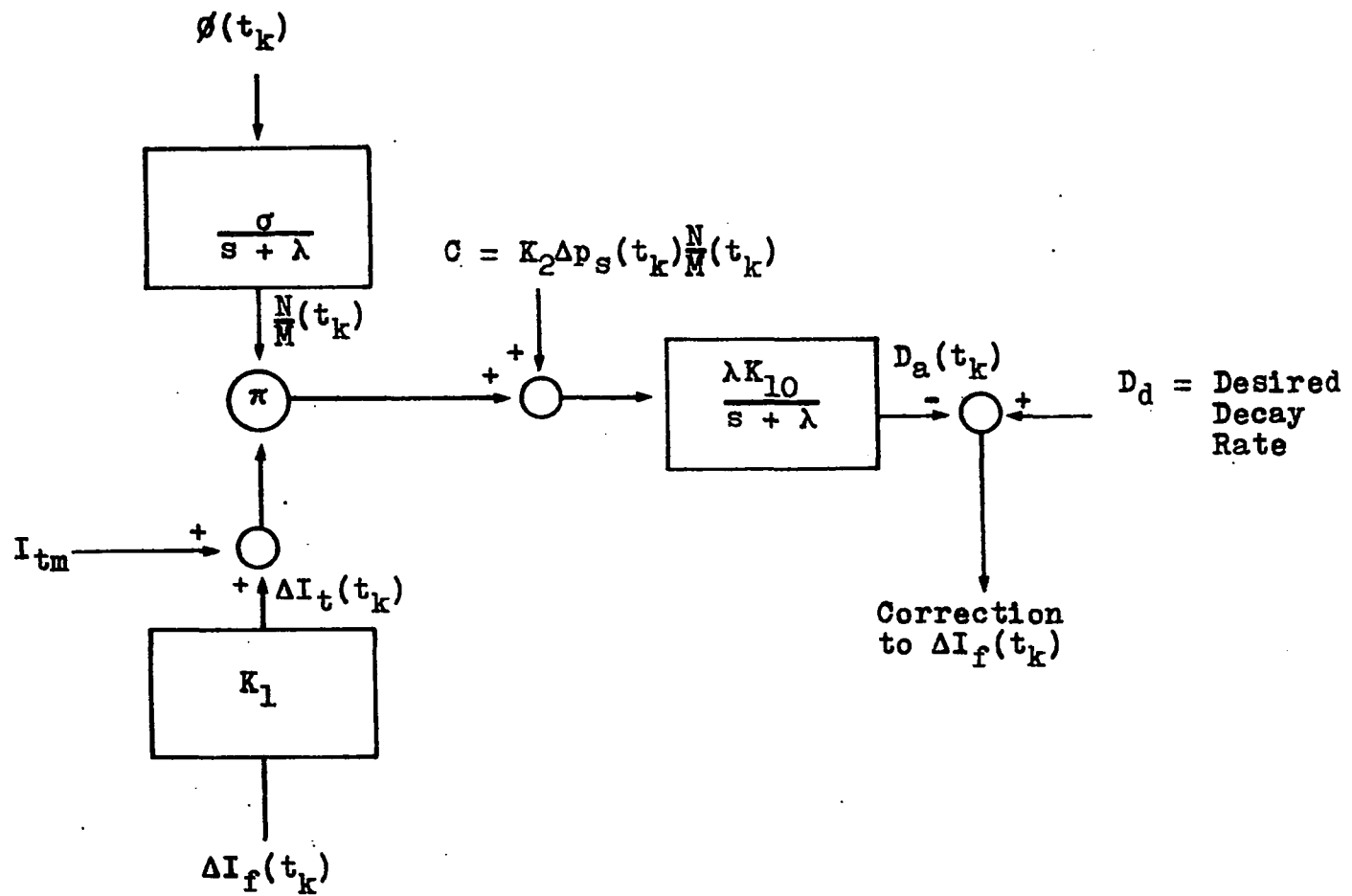


Figure 21. Block diagram of control for ion source filament current

control loop.

These two control loops fix the control system. The control equations require the prediction of approximate solutions for the output states of N/M and D_a and of exact solution of the output state, ΔT_s , in terms of the input current to the sample heater, ΔI_H . These results are shown in the following equations.

$$\frac{N}{M}(t_{k+1}) = e^{-\lambda T} \frac{N}{M}(t_k) + \frac{g}{\lambda}(1 - e^{-\lambda T})\phi(t_k) \quad (64)$$

$$D_a(t_{k+1}) = e^{-\lambda T} D_a(t_k) + K_{10} \left[K_2 \Delta p_s(t_k) \frac{N}{M}(t_k) + \frac{N}{M}(t_k) (K_1 \Delta I_f(t_k) + I_{tm}) \right] (1 - e^{-\lambda T}) \quad (65)$$

$$\Delta T_s(t_{k+1}) = e^{-T/\tau_6} \Delta T_s(t_k) + K_6 \Delta P_H(t_k) (1 - e^{-T/\tau_6}) \quad (66)$$

Using these equations together with the block diagram required values can be obtained for $\Delta P_H(t_k)$ and $\Delta I_f(t_k)$ in terms of the set points, R_d and D_d , the measured and calculated values of the present states, the predicted value of the state of N/M , and known constants. These results are obtained by straightforward algebra. The required values of $\Delta P_H(t_k)$ and $\Delta I_f(t_k)$ to keep constant both the number of radioactive atoms per second vaporized in the sample and the number of radioactive atoms per second decaying at the target are obtained as follows:

$$R_d - \frac{N}{M}(t_{k+1}) [\omega_m + \Delta\omega(t_{k+1})] = 0 \quad (67)$$

Since

$$\Delta\omega(t_{k+1}) = K_8 \Delta T_s(t_{k+1}) \quad (68)$$

the control equation for the first loop is obtained by combining Equation 66, 67, and 68 and solving for $\Delta P_H(t_k)_{\text{req.}}$.

$$\begin{aligned} \Delta P_H(t_k)_{\text{req.}} = & \frac{R_d}{K_6 K_8 (1 - e^{-T/\tau_6}) \frac{N}{M}(t_{k+1})} - \frac{\omega_m}{K_6 K_8 (1 - e^{-T/\tau_6})} \\ & - \frac{e^{-T/\tau_6} \Delta T_s(t_k)}{K_6 (1 - e^{-T/\tau_6})} \end{aligned} \quad (69)$$

First, $\frac{N}{M}(t_{k+1})$ must be predicted and the Equation 69 must be calculated.

For the second loop, the control block diagram indicates

$$D_d - D_a(t_{k+1}) = 0 \quad (70)$$

which together with Equation 65, gives

$$\begin{aligned} D_d - \{ e^{-\lambda T} D_a(t_k) + K_{10} [K_2 \Delta p_s(t_k) \frac{N}{M}(t_k) \\ + \frac{N}{M}(t_k) (K_1 \Delta I_f(t_k) + I_{tm})] (1 - e^{-\lambda T}) \} = 0 \end{aligned} \quad (71)$$

Solving for the required $\Delta I_f(t_k)$ to make Equation 71 valid gives the control equation

$$\Delta I_f(t_k)_{\text{req.}} = \frac{D_d - e^{-\lambda T} D_a(t_k)}{K_1 K_{10} (1 - e^{-\lambda T}) \frac{N}{M}(t_k)} - \frac{K_2}{K_1} \Delta p_s(t_k) - \frac{I_{tm}}{K_1} \quad (72)$$

2. Application of adaptive sampling

According to the adaptive sampling procedure the operation of the experiment is divided into classes according to sampling requirements. The first step is to determine the types of waveforms that can be expected as inputs to each unit block. The second step is to select the design curves from Section III-B-2 according to the expected input and to the measurability (accessibility or inaccessibility) of the output state. The graphs are used to estimate the error caused by the approximation of the predicted output state by piecewise constant inputs if the input is time varying during the sample interval. Since controlled inputs are held constant during a sample interval, they can be predicted exactly for an accurate mathematical model. Errors due to the approximated mathematical model in the system and to unrepresented disturbances that might occur in the system can also influence the choice of sample rate.

The physics experiment control system has been divided into five modes of operation. The considerations and requirements for entering and leaving each mode, the calculations and measurements required for each mode and the error investigation to establish the sample period for measurement and

control are discussed in the following sections.

a. Preliminary Operating Mode Conditions required for operating in this mode are that (1) the maximum number of radioactive atoms per second being vaporized from the sample at maximum permissible sample temperature is less than the desired rate for taking data in the experiment and (2) the measured neutron flux is less than 0.1 per cent of that obtained at the sample for full power reactor operation. The first condition indicates that no dynamic control is necessary in this mode. The second condition assures that no calculations are necessary since the buildup of radioactivity in the sample is negligible compared to that at full power operation. The only measurement necessary in this mode is that of the neutron flux.

The sample period for this mode is chosen to fulfill the requirement that the neutron flux not be allowed to go significantly higher than 1 per cent of full power without being able to switch to the next mode. The reactor normally will go up in power on a positive exponential during a normal startup at no faster than a 30 second "period," i.e., $\tau_p = 30$ seconds. The power can go up a factor of 10 between samples and still meet the required specification. The sample period need be no shorter than 90 seconds to satisfy this requirement. Since this is a trivial computation time for the computer, making the sample period some smaller number, such as 30 seconds,

might be desirable. The mode is shifted to the Startup Mode when the neutron flux is found to be greater than 0.1 per cent of that of full reactor power for a given sample.

b. Startup Mode Conditions required for operating in this mode are that (1) the maximum number of radioactive atoms per second being vaporized from the sample at maximum permissible sample temperature is less than the desired rate for taking data in the experiment and (2) the measured neutron flux is greater than 0.1 per cent of that obtained at the sample for full power reactor operation. The first condition indicates that no dynamic control is necessary in this mode. The second condition indicates that calculations are necessary to allow keeping track of the number of radioactive atoms generated in the sample by the neutron flux. The only measurement necessary in this mode is the neutron flux.

The ratio of radioactive to non-radioactive atoms in the sample is calculated by using Equation 64. A constant has been previously calculated in the computer for the number of atoms per second vaporized when the sample is at the maximum permissible temperature. When this constant is multiplied by the results of the first calculation and then is compared to the desired number of radioactive atoms per second for the given experiment, a decision can be made whether or not to take data.

The sample rate in this mode depends on the error that is

acceptable in the calculation of the ratio of radioactive atoms to non-radioactive atoms in the sample. This output state is inaccessible, and the input is time varying between sample periods. The maximum positive exponential period expected is still 30 seconds as indicated in the Preliminary Operating Mode. For an example, a sample with a radioactive half life of 15 seconds has $\tau_1 = 15$ seconds, $\tau_p = 30$ seconds and $\tau_1/\tau_p = 0.5$ with an acceptable error being 10 per cent. The design graph for this group of parameters is found in Figure 10. From the graph the ratio T/τ_1 is found to be 0.64 for this case. Solving for T , the sample period is found to be 19.4 seconds. For a second example, a sample with a radioactive half life of 1000 seconds has $\tau_1 = 1000$ seconds, $\tau_p = 30$ seconds and $\tau_1/\tau_p = 33$ with an acceptable error still being 10 per cent. The design graph for this group of parameters is found in Figure 11. From the graph the ratio T/τ_1 is found to be 0.02 for this case. Solving for T , the sample period is determined to be 20 seconds. The similarity of the sample periods for the same inputs does not always hold true, since the shapes of the curves vary. The error of 10 per cent is a maximum value and holds as long as the reactor is on the 30 second period. As the reactor period becomes longer the error is reduced until at level reactor power the error will disappear.

The mode is shifted to the Transient Two Level Control

Mode if or when the radioactive atoms per second being vaporized are sufficient in number to take data. The mode is shifted back to the Preliminary Operating Mode if both the number of radioactive atoms being vaporized is insufficient and the reactor power drops below 0.1 per cent of full power.

c. Transient Two Level Control Mode Conditions

required for operating in this mode are that (1) the number of radioactive atoms per second being vaporized from the sample is sufficient to allow data to be taken for a sample temperature within normal operating limits and (2) the calculated value for N/M is more than 3 per cent higher or lower than the saturated activity at the measured neutron flux. This mode of operation requires control for the most dynamic condition of the experiment. The neutron flux may be varying and the radioactivity in the sample has not built up to saturation level. The measurements required for use in the calculations are the neutron flux, the incremental sample temperature, the incremental sample heater current, the incremental pressure at the ion source inlet, the incremental ion source filament current, and the decay rate of the radioactive atoms at the separator target.

The control block diagrams used in this mode are those shown in Figures 20 and 21. The calculations are those shown in Equations 64, 69, and 72 and any conversions necessary to transmit the correction to the experiment in a proper form.

Two specific inputs of the neutron flux variation with time will be considered, the same positive exponential input used in the first two modes and the effect of moving control rods into the reactor for fifty seconds creating a ramp in the neutron flux with a slope of 1 per cent/second. The exponential increase results in the same error as found in the previous modes assuming the error of 10 per cent is still satisfactory. For the half life of $\tau_1 = 15$ seconds the sample period was found to be 10.4 seconds. The design graph for use with the ramp input is found in Figure 2. This graph is used by picking a value of sample period and finding the deviation resulting. For convenience the period is chosen as 19.4 seconds to see if the deviation gives a greater error than the exponential signal did. The ramp will last for 50 seconds which is less than three sample periods. The amplitude deviation/T for $t = 3$ and $T/\tau_1 = 0.64$ is found to be 0.45. The per cent error compared to the initial amplitude of unity is given by

$$\text{Per cent error} = \frac{(\text{Amplitude deviation}/T) \times \text{Ramp gain} \times 100}{\text{Initial Amplitude}}$$

Using the parameters above gives

$$\text{Per cent error} = \frac{0.45 \times 19.4 \times 0.01 \times 100}{1} = 8.7\%$$

This is no greater than the error caused by the positive exponential so is consistent for the original requirement for

an error of less than 10 per cent.

The mode is shifted to the Transient One Level Control Mode if or when the calculated value of N/M deviates less than 3 per cent from the saturated value at the measured neutron flux. The mode is shifted back to the Startup Mode if there are insufficient radioactive atoms with which to take data.

d. Transient One Level Control Mode Conditions

required for operating in this mode are that (1) the neutron flux must not change more than 5 per cent from that when the mode was entered and (2) the ion source filament current must be in a proper operating range for control. The latter requirement is implicit in all modes of operation using control but is emphasized here since any variation in N/M due to change in neutron flux now must be corrected by the ion source filament current, instead of through changing the sample heater current. This mode has less dynamic range of operation than the previous one since the time history of the neutron flux and the buildup of radioactivity in the sample has become reasonably stable. The measurements required for use in the calculations are the neutron flux, the incremental pressure at the ion source inlet, the incremental ion source filament current, and the decay rate of the radioactive atoms at the separator target.

The control block diagram used in this mode is that shown in Figure 21. The value of C can now be time varying over a

small range of operation since control is no longer being maintained in the control loop shown in Figure 20. The calculations are those shown in Equations 64 and 72 and any conversions necessary to transmit the correction in an appropriate form to the experiment.

The neutron flux does not vary significantly in this mode of operation so approximation errors are small. There can be small, step inputs of neutron flux for slight repositioning of control rods for shimming purposes. Any change of neutron flux greater than 5 per cent will shift operation out of the mode. The control provides the last trimming of operation as the experiment and reactor are coming into a stable, steady state operation. The mode is shifted to the Transient Two Level Control Mode if the neutron flux varies more than 5 per cent from that flux with which the mode was entered or if the ion source filament current reaches the limit of its operating range.

e. Monitor Mode The reactor and the experiment may reach a very stable mode of operation requiring little or no correction in the experiment control to maintain satisfactory experimental conditions. If this condition occurs the computer should not be called upon to make calculations that are no longer required. If the graphs were used to calculate errors from expected deviations, the sample period would turn out to be very long. Disturbances or changes in between

samples become a distinct possibility. The occurrence of such changes early in the sample period could cause considerable deviation before the next sample measurement.

The Monitor Mode is operated by a function of the computer referred to as a Clock Interrupt. The Clock Interrupt is an automatic callback for quick interrogation of experiment conditions requiring very little calculation time at regular periods of time. These clock periods start at 12.8 milliseconds and are available at other longer periods. This shorter sample period would perform no control but would check the values of the three most critical variables, the neutron flux, the total isotope separator current and the decay rate of the radioactive nuclides at the isotope separator target. Any significant drift from their values when the Monitor Mode was entered will cause the operation to shift back either to the Transient One Level Control Mode or the Transient Two Level Control Mode, depending on which mode is required.

V. CONCLUSIONS AND RECOMMENDATIONS

The design curves from this study provide a means for design of effective control for an experiment and at the same time assist in making efficient use of a digital computer shared by other experiments. The state variable technique is used as both a design method for obtaining the design curves for adaptive sampling and for predicting the state for the control of the system. The ease with which the state variable technique accommodates changing sample intervals shows why the technique is able to unify examination of non-uniform, aperiodic, and constant interval sampling methods. The method of adaptive sampling developed here is shown to be easily applied whether the states of the process are measurable (accessible states) or not measurable (inaccessible states).

An interesting and useful characteristic is demonstrated for process systems which have particles or components that originate at the input of the process, are carried through the process in space and time and finally are expelled from the process never to return. These processes are commonly described by a set of nonlinear differential equations with time-varying coefficients. Solving this set of equations simultaneously is both a long and difficult task. For processes with the characteristics described above this set of nonlinear differential equations can be uncoupled and the

resulting sets solved in sequence. In the experiment on which the adaptive sampling is demonstrated the set of uncoupled equations prove to be individual first order differential equations that are linear.

System control can be changed in the digital computer by merely replacing the program stored in the computer, demonstrating one of the major advantages the digital computer has over an analog system designed to provide the same control. If the required control program is already stored in the computer, the control system can be changed in a time that is short compared to the time constants of the process. The stored programs can be changed to new programs with a minimum of time and effort when the experiment is changed. The pre-stored program potentially provides a wide dynamic range for a given process that seems highly unlikely to be accomplished even by an adaptive analog control system.

Further development of the adaptive sampling technique is desirable. A more sophisticated method can be developed for making the decision to change from one mode to another. The method here uses the magnitudes of the state variables and the inputs to the process for mode switching decisions. The derivatives of each state are available with little additional calculations. The rate of change of the state variables would give an added anticipation of a need for greater attention from the computer. The development of the combination of

clock interrupts for monitoring and experimental interrupts for control appears to be one of the most fruitful areas for further development. A good balance between these two functions could reduce even further the demands on the digital computer by a process with given control specifications. The investigation of stability was mentioned only briefly. Stability and optimum control studies open wide the avenues of research using the techniques discussed here.

VI. BIBLIOGRAPHY

1. Bellman, Richard. Adaptive control process: a guided tour. Princeton, New Jersey, Princeton University Press. 1961.
2. Bellman, Richard and Kalaba, R. Dynamic programming and adaptive processes. Institute of Radio Engineers Transactions on Automatic Control AC-5:5-10. 1960.
3. Brown, R. G. and Nilsson, J. W. Introduction to linear systems analysis. New York, N. Y., John Wiley and Sons, Inc. 1962.
4. Chestnut, H., Sollicito, W. E. and Troutman, P. H. Predictive control system application. American Institute of Electrical Engineers Transactions 80, Part 2:128-139. 1961.
5. Fuller, A. T. Phase space in the theory of optimum control. Journal of Electronics and Control 8:381-400. 1960.
6. Gupta, S. C. and Hasdorff, L. Changing the state of a linear system by use of normal function and its derivatives. Journal of Electronics and Control 14, No. 3: 351-359. 1963.
7. Henrici, Peter. Discrete variable methods in ordinary differential equations. New York, N. Y., John Wiley and Sons, Inc. 1961.
8. Hoag, J. Barton. Nuclear reactor experiments. Princeton, New Jersey, D. Van Nostrand Company. 1958.
9. Hufnagel, R. E. Analysis of aperiodically sampled data feedback control systems. Unpublished Ph.D. thesis. Ithaca, New York, Library, Cornell University. 1959.
10. Kalman, R. E. and Bertram, J. E. General synthesis procedure for computer control of single and multiloop systems. American Institute of Electrical Engineers Transactions 77, Part 2:602-609. 1959.
11. Kalman, R. E. and Bertram, J. E. A unified approach to the theory of sampling systems. Franklin Institute Journal 267:405-436. 1959.

12. Kuo, Benjamin C. Analysis and synthesis of sampled-data control systems. New York, N. Y., Prentice Hall, Inc. 1963.
13. Loomis, Robert H. Decoupling techniques in multiloop control systems. Institute of Radio Engineers International Convention Record 8, Part 4:53-63. 1960.
14. Meditch, J. S. and Gibson, J. E. Real time control of time-varying linear systems. Institute of Radio Engineers Transactions on Automatic Control AC-7, No. 4:4-9. 1962.
15. Merriam, C. W., III. A class of optimum control systems. Franklin Institute Journal 267:267-281. 1959.
16. Monroe, Alfred J. Digital processes for sampled data systems. New York, N. Y., John Wiley and Sons, Inc. 1962.
17. Pearson, J. D. Approximation methods in optimal control. I. Sub-optimal control. Journal of Electronics and Control 13, No. 5:453-469. 1962.
18. Ragazzini, J. R. and Franklin, G. F. Sampled data control systems. New York, N. Y., McGraw-Hill Book Co., Inc. 1958.
19. Tou, Julius T. Optimum design of digital control systems. New York, N. Y., Academic Press, Inc. 1963.

VII. ACKNOWLEDGEMENTS

The author wishes to express his appreciation to his major professor, Dr. Robert M. Stewart, for his helpful suggestions and comments, to Dr. Willard L. Talbert for his help in providing the experiment for the practical application, and to the examining committee for their consideration.